Manganese Enzymes with Binuclear Active Sites

G. Charles Dismukes

Hoyt Laboratory, Department of Chemistry, Princeton University, Princeton, New Jersey 08544

Received June 24, 1996 (Revised Manuscript Received September 12, 1996)

Contents

G. Charles Dismukes is Professor of Chemistry at Princeton University, where he has been a member of the faculty since 1978. He received his Ph.D. in physical chemistry for research supervised by John Willard in the field of radiation chemistry at the University of Wisconsin in Madison and did postdoctoral research with Kenneth Sauer and Melvin Klein in the field of photobiology at the University of California in Berkeley. He was a visiting scholar at the Service de Biophysique of the Centre d'Etude Nucleares-Saclay in 1984 and at the Squibb Phrmaceutical Research Institute in 1991. He has received the Searle Scholars Award, 1981–1983, Alfred P. Sloane Award, 1984–1986, and a Japan Society for the Promotion of Science Award, 1992. His current research interests including structure and mechanisms of multimetal containing enzymes and bio-inspired inorganic catalysts.

I. Introduction

The purpose of this article is twofold. First, to review the recent literature dealing with the mechanisms of catalysis by binuclear manganese enzymes. Second, to summarize and illustrate the general principles of catalysis which distinguish binuclear metalloenzymes from monometallic centers. This review covers primarily the published literature from 1991 up to May 1996.

A summary of the major structurally characterized dimanganese enzymes is given in Table I.1. These perform various reaction types including several redox reactions, (de)hydrations, isomerizations, (de)-phosphorylation, and phosphoryl transfer. Several of the manganoenzymes listed in Table I.1 have not been further characterized in the last five years and will not be discussed further here. These include thiosulfate-oxidizing enzyme and bacterial ribonucleotide reductase. The reader should consult the earlier reviews noted below for references to this literature. The tetramanganese core which catalyzes photosynthetic oxygen production from water is the subject of a separate review in this volume by Klein, Sauer, and Yachandra and will also not be discussed here. Recent crystallographic studies and a kinetics study of xylose isomerase have lead to a modification of the proposed mechanism for this isomerization reaction which can be found in the original literature.[1−4] Earlier reviews of binuclear Mn enzymes can be found in the works by Markham,[5] Que and True,[6,7] Dismukes,[8,9] and Kessissoglou.[10] There is extensive literature on synthetic models of manganese enzymes and reactions of Mn with dioxygen and its reduced derivatives that will not be reviewed here. Some specialized reviews may be consulted for this purpose.[11−15]

Some of the enzymes listed in Table I.1 function only with manganese at the active site, notably the redox class of enzymes, while others such as the hydrolytic class often are active with various divalent ions. Mg^{2+} is often the endogenous metal ion associated with the hydrolytic enzymes as isolated. This includes xylsose isomerase, most exonucleases, ribonuclease H, and enolase. The active form of phosphotriesterase as isolated from *Pseudomonas* and *Flavobacteria* contains 2 equiv of Zn^{2+} bound to the active site. The activity of these enzymes with Mn^{2+}

S0009-2665(95)00053-7 CCC: $25.00

Table I.1. Multinuclear Manganese Enzymes

enzyme	Mn_x site Mn−Mn, Å	net reaction	enzyme reaction	distribution
arginase	binuclear Mn^{II}−X−Mn^{II}	arginine → urea + ornithine	hydration of guanidinium group	yeast, bacteria mammals
catalase	binuclear Mn^{II}−X−Mn^{II}, 3.6 Å	$2H_2O_2 \rightarrow O_2 + 2H_2O$	redox, Mn^{II}, Mn^{III}	thermophillic and heme deficient bacteria
thiosulfate-oxidizing	binuclear Mn^{II}−X−Mn^{II}	$S_2O_3^{2-} \rightarrow SO_4^{2-}$	presumed redox	thiobacilli
ribonucleotide reductase	presumed binuclear Mn^{III}−O−Mn^{III}	ribonucleotides → deoxyribonucleotides	tyrosine → tyrosyl radical	bacterial
photosynthetic water oxidase	tetranuclear $Mn(O)_2Mn$, 2.7 Å; Mn−X−Mn, 3.3 Å	$2H_2O \rightarrow O_2 + 4e^- + 4H^+$	redox, Mn^{III}, Mn^{IV}	plants, algae
xylose isomerase	binuclear $Mn^{II}(RCO_2)Mn^{II}$ 4.9 Å	glucose → fructose	1,2-keto−alcohol isomerization	bacterial
3′−5′ exonuclease	binuclear $Mn^{II}(RCO_2)Mn^{II}$, 4 Å, Mg or Mn	DNA + H_2O → cleaved DNA	phosphodiester hydrolysis	bacterial, diverse
ribonuclease H	binuclear $Mn^{II}(RCO_2)Mn^{II}$, 4 Å, Mg or Mn	RNA + H_2O → cleaved RNA	phosphodiester hydrolysis	retrovirus, bacterial
phosphotriesterase	binuclear $Mn^{II}(RNHCO_2)(OH_2)Mn^{II}$, 4 Å, various M^{2+}	phosphotriester → alcohol + phosphodiester	phosphotriester hydrolysis	bacterial
dinitrogen reductase regulatory protein (DRAG)	binuclear Mn^{II}−X−Mn^{II}	peptide arginyl-ADP → peptide arginine + ADP	phosphoamide hydrolysis	bacterial
enolase	binuclear $Mn^{II}(RCO_2)Mn^{II}$ E·S complex, Mg or Mn	glycolysis: 2-PGA → P-enolpyruvate	reversible hydration of C=C	all eukaryotes

replacing the endogenous divalent cation is generally comparable and on this basis thought to operate by identical mechanisms. Native manganese-containing hydrolytic enzymes include liver arginase and dinitrogen reductase regulatory protein. Hydrolytic metalloenzymes can often employ divalent metal ions with similar physicochemical properties such as ionic radius, hydration free energy and Lewis acidity because they are involved in essentially electrostatic activation of a substrate or water molecule. These properties are similar for Mg^{2+} and Mn^{2+} (0.7 vs 0.8 Å; −1895 vs −1820 kJ/mol; pK_a = 10.6 vs 11.4).[16,17] By contrast, the redox class of manganoenzymes perform various oxidation/reduction reactions involving more specific functions, such as the delivery of one or more electrons at a specific electrochemical potential and in some cases including oxo transfer. These processes will be both metal specific and oxidation state specific. Several examples are found in nature of manganoproteins and manganoenzymes containing Mn^{2+}, Mn^{3+}, and Mn^{4+}.

For the purpose of this article binuclear metal centers in enzymes are defined in structural terms as those which share a common bridging ligand derived either from solvent, an amino acid residue from a protein or a nucleoside from DNA or RNA. Another important distinction of binuclear metal centers is the occurrence of electronic coupling between the metals, in contrast to sites containing two uncoupled metal ions. This bonding can involve both ionic and covalent interactions that are mediated by direct metal−metal forces or through the ligands or solvent.

II. General Concepts of Catalysis by Binuclear Metal Sites

Why do some enzymes employ binuclear metal sites for hydrolysis or redox reactions, whereas others work quite well with mononuclear metal sites? For example, why has Nature selectively employed dimanganese catalases in certain bacteria as well as the widely distributed monoiron heme-type catalases? And why do dimanganese hydrolases like arginase exist as well as the monozinc-dependent hydrolases? One notion is that the two metals work more or less independently, being required for distinct functions either structural or catalytic, or alternatively, catalyzing different steps in a multistep sequence. Some heterobimetallic centers do appear to employ the two metals in different functions. Possible examples being the CuZn superoxide dismutase and the FeZn purple acid phosphatase.[18,19] However, even in such cases it is clear that the distinct functions are not independent; there is interaction between the sites that is essential for catalysis. The metal ions in a bimetallic center usually exhibit strongly correlated physicochemical properties, in cases where they share a monoatomic or conjugated bridging ligand (i.e., μ-aqua, μ-hydroxo, μ-oxo), particularly when they possess uncompensated (net) charges. By contrast, the individual metal ions in a bimetallic center can exhibit independent physicochemical properties in cases where the metal ions are decoupled by larger polyatomic bridging ligands which also electrostatically screen the metals (i.e., μ-carboxylate, μ-imidazolate). A defining feature of the uncoupling of the metal ions is the observation that binuclear centers can undergo apparently simultaneous two-electron redox transitions at a single electrochemical potential. In mononuclear metal centers two-electron steps are also possible, but must be accompanied by compensating changes in the ligand field potential or proton ionization which creates the same or nearly the same electrochemical potential for the individual one-electron steps. Homobimetallic centers have the additional feature of symmetric delocalized charge distributions that can operate together as a unit to enable stabilization of transition states involving concerted steps, such as nucleophillic ligand substitution reactions (S_N2 chemical nomenclature) in which simultaneous anionic ligand addition and anionic ligand dissociation require electrostatic stabilization.

A. Catalysis of Redox and Hydrolytic Reactions by Binuclear Centers

Binuclear sites in enzymes appear to have several potentially useful properties either not found or deficient in mononuclear centers which could be important for catalysis. These include:

(1) Charge delocalization over two centers vs one metal facilitates two-electron redox reactions that would require a larger thermodynamic driving force in a mononuclear center.[20] Examples include hemerythrin, myohemerythrin,[21] and Mn catalase.

(2) Activation barriers arising from nuclear reorganization of the solvent and the surrounding medium (enzyme) can be less in binuclear vs mononuclear centers having the same net charge, owing to greater charge delocalization. However, the bridging position between the metal ions has a larger electrostatic potential. If this site is where the substrate binds then substrate activation through bond polarization can be achieved and used for catalysis.

(3) Opportunities for gating of the redox potential upon binding of substrate offers a means for protecting the active site from premature redox reactions which can often be destructive (i.e., methane monooxygenase and Mn catalase). There are more opportunities for protein-mediated gating mechanisms in binuclear centers, owing to the larger number of potential interaction pathways (ligands). For example, in Mn catalase the strong oxidizing potential of the (III,III) oxidation state is effectively unavailable for destructive side reactions owing to the much faster rate of reduction by peroxide than the rate of formation by peroxide. Thus, at all concentrations of peroxide in the medium the majority species is the unreactive (II,II) oxidation state.

(4) Polyatomic substrates which require activation by binding at more than one atom can generally be accommodated better at binuclear centers.

(5) Electrostatic activation of substrate or ionization of a proton from an active-site water molecule will occur more readily at a charged binuclear center, $[M_2]^{2n+}$ than at the corresponding mononuclear center M^{n+} (i.e., arginase, enolase, xylose isomerase, exonuclease, RNase H). The estimated binuclear electrostatic effect is worth about 3.4 pK units to the free energy of dissociation of a proton from a water ligand compared to the corresponding mononuclear aqua Mn^{2+} species.[22]

(6) Formation of a low-energy transition state, for example the negatively charged trigonal-bipyramidal transition state formed during phosphodiester bond hydrolysis (−2 net charge) by nucleases and RNase H, is predicted to be energetically favored by symmetrical coordination of the axial ligands to the metal ions of a binuclear center. This geometry is achieved in exonucleases via formation of two bidentate bridges involving an equatorial phosphate O atom.[23] This "binuclear effect" lowers the activation barrier to both nucleophile attack and phosphoester bond cleavage.[24]

(7) Studies of the change in ligand field potential of Mn(II) observed via zero-field splittings (ZFS) in the EPR spectra of model complexes indicate that the second metal ion in binuclear complexes attenuates the strength of the bridging-ligand field potential. A weakened bridging-ligand field potential may play a functional role in increasing the oxidation potential or increasing the binding affinity to other ligands such as water, thereby increasing the Lewis acidity. For example, in promoting ionization of a proton from a manganese-bound water molecule in arginase, with the resulting hydroxide ligand serving as the nucleophile needed for hydrolysis of substrate.

Several of these concepts will be highlighted in section III using dimanganese enzymes as examples.

B. The μ-Carboxylate Conundrum: Passive Structural or Redox Decoupling Function?

A common structural feature found in most binuclear proteins and enzymes is the presence of one or two bridging (μ) carboxylates derived from aspartate or glutamate side chains of the protein. These commonly adopt μ-1,3 geometry in which each O atom is coordinated to different metal ions, Chart II.B.1. Another geometry involving nonsymmetrical

Chart II.B.1

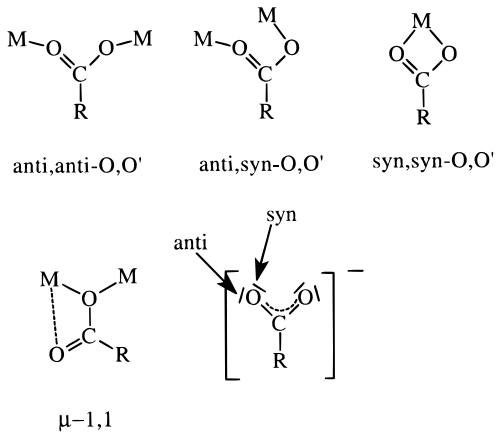

μ-1,1 coordination has also been found in some bimetallic complexes and enzymes.[25] Because there are two lone pairs on each O atom which can participate in metal bonding, designated as *syn* and *anti*, two forms of the μ-1,3 bridging geometry can be realized, *anti*,*anti*-O,O′ or *anti*,*syn*-O,O′, Chart II.B.1. Examples exist of each of these in inorganic complexes, but their occurrence in proteins is not so clear due largely to poorer resolution of the X-ray structures. There is also the syn−syn geometry which can accommodate only a single metal ion and is commonly referred to as bidentate.

The possibility of interconversion between the μ-1,3 and μ-1,1 geometries is one example of a rearrangement that has been termed the carboxylate shift.[26] This shift is thought to be important for allowing expansion of the coordination sphere in cases where substrate binding is coupled to redox cycling of the metal center, and as such would also include rearrangement of terminal carboxyl ligands between bidentate and monodentate geometries on a single metal.

The occurrence of μ-1,3-carboxylates appears to be a universal feature of bimetalloproteins and complexes which perform two-electron or multielectron chemistry. This correlation has been proposed to have a functional significance beyond the obvious structural necessity; the contrasting views have been termed the μ-carboxylate conundrum.[27,55] Several examples of μ-1,3-carboxylate-bridged binuclear enzymes which perform two-electron concerted oxidations and suppress discrete one-electron steps are given in eqs 1a−d. These include O_2 binding by hemerythrin, eq 1a;[28] peroxy intermediate formation by methane monooxygenase, eq 1b (proposed struc-

ture);[25,29] oxidation of the diferrous intermediate by O_2 during the assembly of ribonucleotide reductase, eq 1c;[30] and peroxide dismutation by Mn catalase, eq 1d.[8,31] All of these enzymes possess carboxylate-

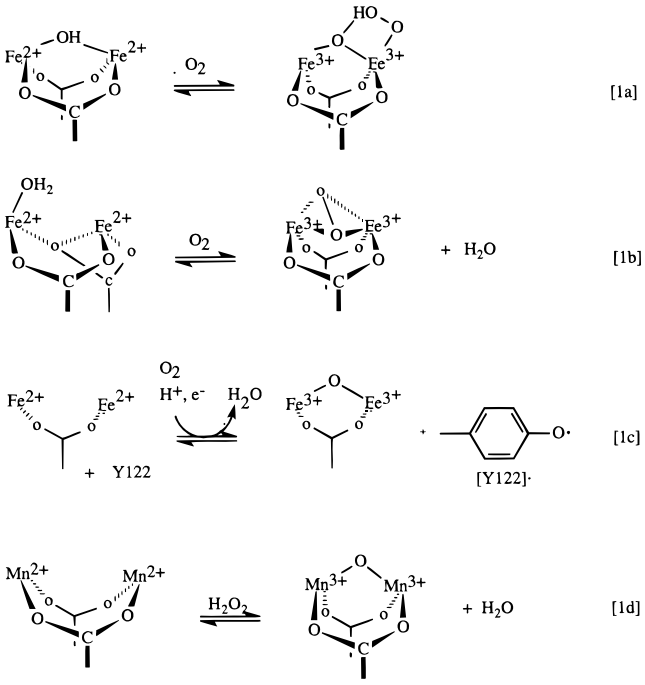

bridged bimetallic centers, in which both metal ions participate more or less equally in providing the electrons, as judged by a variety of physicochemical experiments.

Bridging carboxylates probably serve a functional role beyond merely that of a passive structural bridge to bring the metal ions together. Their size and negative charge enables them to spatially separate and electrically screen the metal ions so that the degree of intermetallic electronic coupling is small. $Mn_2^{II,II}(\mu\text{-carboxylate})_{1-2}$ complexes are relevant examples with weak electronic coupling. An important consequence of this uncoupling is that the electronic degeneracy that is intrinsic to symmetrical homobimetallic sites is not lifted through Jahn−Teller distortions. In other words, there is negligible vibronic coupling between the electronic energy and the (asymmetric) nuclear distortions (vibrations) that in cases of single ions with degenerate states, like Mn(III), could couple strongly to produce valence trapping. This uncoupling of the Mn(II) ions from small amplitude vibrations of the bridging carboxylate results in both metal ions undergoing oxidation at close to the same electrochemical potential. In contrast to terminally bound ligands, μ-1,3-carboxylates interact directly only with the two metal ions and are isolated from the surrounding environment. Replacement of the μ-1,3-carboxylate by small monoatomic anions or ionizable water (hydroxide) ligands leads to stronger electronic interaction between the metal centers and also with the environment or substrate via hydrogen bonding or proton ionization. This stronger vibronic coupling results in separation of the redox couples into well-resolved one-electron steps with formation of the mixed-valence species becoming possible with one-electron donors or acceptors. A case in point is Mn catalase where formation of both the Mn_2(II,III) and Mn_2(III,IV) oxidation states occurs readily when starting from the μ-oxo-μ-carboxylate-Mn_2(III,III) state, while oxidation of the reduced μ-carboxylate-Mn_2(II,II) state, which lacks the μ-oxo, occurs by a two-electron process.

This μ-carboxylate concept is illustrated by the electrochemical data on complex **1**, $[LMn_2(\mu\text{-OAc})](ClO_4)_2$, and its isostructural μ-chloroacetato derivative vs the derivatives, LMn_2Cl_3 (**2**) and $LMn_2(OH)Br_2$ (**3**), which have the μ-carboxylato replaced by μ-Cl^- and μ-OH^-, respectively. These data reveal that only the μ-carboxylato derivatives fail to exhibit a one-electron redox pathway leading to the mixed-valence species Mn_2(II,III), in contrast to species **2** (E_0 = 0.49 V) and **3** (0.54 V).[32,33] Replacement of μ-Cl^- or μ-OH^- by μ-carboxylato or μ-chloroacetate increases the reduction potential for the one-electron process by *ca.* 0.3−0.35 V up to the same potential as the second electron step at 0.8−0.85 V. This results in the simultaneous two-electron process Mn_2(III,III) ↔ Mn_2(II,II) becoming favored over sequential one-electron steps at different potentials.

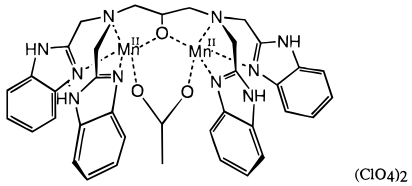

1

For Mn catalases *in vivo* suppression of the mixed-valence Mn_2(II,III) state is absolutely critical for proper functioning and presumably cell viability. The mixed-valence state does not form during enzymatic turnover, but can be induced artificially as an intermediate during reduction with hydroxylamine, iodide, and other one-electron reductants.[34] If this partial reduction is allowed to occur in the presence of peroxide the intermediate can be quantitatively oxidized to a catalytically inactive di-μ-oxo-Mn_2(III,IV) species.[34,35] Although this "superoxidized" state can be fully reactivated by reductants, reduction occurs so slowly (half-time ∼30 min) as to render the enzyme effectively unavailable during the cell's lifetime. Consequently, redox chemistry which forms either of the mixed-valence species must be strongly selected against by the organism.

The Bridging-Ligand Field Potential. The redox potentials for transfer of electrons to and from a metal ion are directly influenced by the type of ligands which are bound to the metal. The zero-field splitting (ZFS) of a paramagnetic ion provides a measure of the asymmetry in the ligand field potential, and can be used to estimate the change of the ligand field strength in a series of metal−ligand complexes. Comparison of the change in the magnitude of the ZFS in Mn(II) model complexes and dimanganese(II,II) enzymes indicates that the second metal ion in binuclear complexes possessing a shared bridging ligand (O^{2-}, OH^-, RO^-) attenuates the strength of the bridging-ligand field potential. An empirically observed linear correlation has been found between the axial component of the ligand field induced single-ion zero-field splitting parameter $|D_c|$ and the intermanganese distance in a series of ligand-bridged dimanganese(II,II) complexes and

proteins, including alkaline phosphatase and concanavilin A.[31] A reduced value of $|D_C|$ was found to correlate linearly with shorter intermanganese distances. A factor of 2−4 reduction was observed relative to the corresponding single-ion Mn^{2+} complexes. That such a correlation exists should not be surprising, since the bridging-ligand field strength at both ions must decrease as the metal ions approach one another, assuming no other changes in the nonbridging ligands were to occur. The useful insight to take from this correlation is that it establishes that the intermanganese separation contributes in a significant way to the asymmetry of the ligand field potential and can be measured via the ZFS parameter. Accordingly, motion along this coordinate is an important means for activation of substrate molecules through electrical polarization. Mn catalase is an example where the intermanganese separation is known to change in response to anion binding at the active site.[36,37]

The weakened bridging-ligand field potential in a binuclear center will increase the reduction potential of the metal site (more electropositive metals), if bonding to the remaining ligands were to remain unaffected. Relaxation of the remaining ligands around the slightly more electropositive metal ions corresponds to stronger ligand−metal binding and the possibility to increase the Lewis acidity of these ligands. This can be used, for example, in promoting ionization of a proton from a manganese-bound water molecule in arginase, with the resulting hydroxide ligand functioning as the nucleophile needed for hydrolysis of substrate. This bridging-ligand mechanism operates in addition to the direct electrostatic mechanism proposed above for the second metal ion. A reduced bridging-ligand field is presumed to be responsible for the weakening of the bond between Cu^+ and its μ-histidine ligand that bridges to Zn^{2+} in superoxide dismutase. Dissociation of the μ-imidazolate-Zn^{2+} from Cu^+ occurs following reduction of Cu^{2+} in SOD and is accompanied by protonation of imidazolate. This process appears to play an essential role in proton delivery to form product hydrogen peroxide.[18]

III. Dimanganese Enzymes

A. Arginase

1. L-Arginine Hydrolysis

L-Arginine, one of 21 amino acids utilized by living cells for protein biosynthesis, also serves as a key precursor in several major biochemical pathways, including the elimination of nitrogenous excretion products (via the urea cycle) in the biosynthesis of polyamines as growth factors and in intracellular communication via the formation of nitric oxide (NO). The concentration of arginine in many tissues is controlled by the enzyme arginase (L-arginine amidinohydrolase, EC 3.5.3.1). Arginase is utilized in the liver to convert L-arginine to urea and L-ornithine, Figure III.A1. Urea is the principal metabolyte for disposal of nitrogen as a neutral and nontoxic waste product formed during amino acid metabolism in mammals. L-Ornithine serves as a biosynthetic precursor to L-proline and the polyamines. Arginases

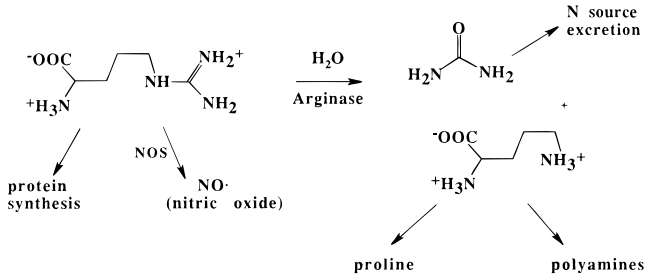

Figure III.A.1. Arginase catalyzes the hydrolysis of L-arginine to urea and ornithine.

are ubiquitous in nature, having been found in bacteria, fungi, plants, reptiles, and mammals. This diversity, exemplified by the presence of the enzyme in organisms which do not require urea, indicates a fundamental importance of arginase in metabolism beyond merely a source of urea and ornithine.

In mammals, arginase has been detected in many different tissues having an incomplete urea cycle, such as red blood cells, brain, kidney, mammary gland, and the gastrointestinal tract, where the principal function is not associated with nitrogen excretion.[38−41] The specific activity of arginase in these tissues is 1−2% of the activity in liver. This diversity is known to be linked to the existence of two isoforms of arginase, so-called AI and AII forms. Genetic evidence indicates that the "liver" (AI) and "kidney" (AII) enzymes are coded by different genes.[42,43] The lack of an abundant source of the AII isozyme has greatly limited molecular studies which could address the question of possible other physiological functions.

Arginase is also a major enzyme in the pathway which produces polyamines such as putrescine, spermine (in eucaryotes), and spermidine (in procaryotes), via decarboxylation of L-ornithine catalyzed by ornithine decarboxylase. These polyamines are found in high concentrations in actively growing cells where they act as growth factors. It is believed that they play a role in controlling rates of nucleic acid biosynthesis. Polyamines also serve to stabilize membrane structures of bacteria, as well as the structure of ribosomes and some viruses. Thus, L-ornithine formation may be the main function of arginase in cells which have incomplete urea cycles.

The best characterized form of arginase comes from the liver (see Note Added in Proof). Rat liver arginase is a homotrimeric protein with molecular mass 35 kDa/su. Each subunit possesses a pair of spin-coupled Mn(II) ions that is required for arginase activity.[44] In the "aqua" form of the enzyme as found at neutral pH the separation of the Mn ions was found to exhibit a distribution of distances, 3.4−3.6 Å, as deduced from the zero-field splitting in the EPR spectrum of the excited quintet state.[31] The distribution of distances narrows in the presence of inhibitors like borate or L-ornithine, yielding a single distance of 3.50 Å, suggesting that these may bind to the active site, perhaps directly to the Mn_2 site. This intermanganese distance is consistent with the likely presence of one or two bridging carboxylate residues. The temperature dependence of the EPR intensity was modeled by fitting to a Boltzmann expression for a pair of Mn(II) ions coupled by isotropic Heisenberg spin exchange ($-2JS_1 \cdot S_2$). This dependence indicates

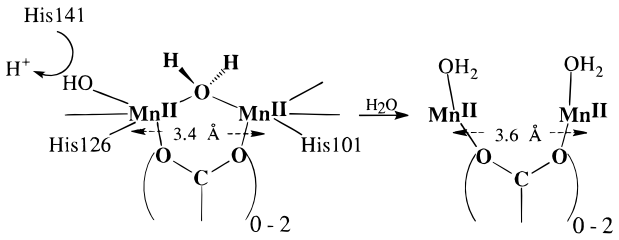

Figure III.A.2. EPR and mutagenesis derived structure of rat liver arginase.

a diamagnetic ground state with triplet−singlet energy gap ΔE_{10} (cm^{-1}) = $|2J|$ = 4 for Mn_2(II,II)Arg-(+borate). This interaction is a factor of 4 smaller than found in Mn_2(II,II) catalase and 6 times smaller than for $[LMn_2(CH_3CO_2)](ClO_4)_2$ (complex **1**) or LMn_2Cl_3 (complex **2**) or $LMn_2(OH)Br_2$ (complex **3**). This large difference in energy gaps reflects either a difference in the bridging ligands, or possibly, a weaker ligand field (larger ionization potential) for the Mn(II) ions in arginase. Comparison of the extremely weak Heisenberg exchange interaction constant with those from more than 30 dimanganese-(II,II) complexes suggests a possible bridging structure with a μ-aqua ligand and one or two μ-carboxylates. These results lead to the preliminary structural model depicted in Figure III.A.2.[31]

The two histidine residues, His101 and His126 depicted in Figure III.A.2, have been proposed as terminal ligands to Mn on the basis of mutagenesis studies in which both conserved residues were mutated to Asn residues.[45] The resulting mutants were found to retain high arginase activity in the presence of exogenous Mn(II), but in the presence of the chelator EDTA less than 0.2% activity was found, as summarized in Table III.A.1. Compared to the wild-type enzyme containing 6 Mn/trimer, the Mn stoichiometry is reduced in both mutants to 3.3 (H101N) and 3.6 (H126N) following dialysis against Chelex-100 ion exchange resin, and to a uniform 3.0 following treatment with the chelator EDTA.

A third highly conserved residue, His141, is not involved in Mn binding, as judged by EPR studies of the H141N mutant.[22] His141 is the site of inhibition of arginase activity upon alkylation with diethyl pyrocarbonate (DEPC). This inhibition is fully reversed by hydroxylamine, which is known to restore the native His by N-dealkylation. His141 is thus implicated as a general base in the mechanism, perhaps responsible for deprotonation of the metal-bound water nucleophile, as depicted in Figure III.A.2.[46] In the proposed mechanism the metal-bound hydroxide functions as the nucleophile which attacks the guanidinium carbon of L-arginine, forming a tetrahedral intermediate which eliminates urea and L-ornithine as the stable products.

Chemical evidence supporting this proposed mechanism has come from studies of competitive inhibition of arginase activity by a series of N^{ω}-hydroxyamino acids.[47] Strong inhibition by N^{ω}-hydroxy-L-lysine was observed, while N^{ω}-hydroxy-L-ornithine exhibits a 37-fold weaker inhibition. The authors proposed that the additional CH_2 unit in L-lysine is critical to allowing interaction with the Mn_2 center, and that the N^{ω}-hydroxyl group may act as a transition state inhibitor by displacement of the metal-bound water nucleophile. According to this model the binuclear metal center serves to ionize the substrate water molecule that hydrolyzes the guanidinium carbon.

Evidence from steady-state kinetics indicates that a protein functional group with pK_a = 7.9−8.0 controls the rate of hydrolysis at the guanidinium carbon of the L-arginine substrate.[46,48] This base is presumed to deprotonate water, forming the hydroxide nucleophile in the active site. This pK_a is 2.7 units lower than that found in mononuclear Mn(II) complexes with neutral ligands such as aquamanganese(II), eq 2a. On this basis arginase is thought to lower the pK_a of a water ligand by forming a binuclear site, and also by coordination of Mn(II) to Lewis acidic ligands.

The increase in the Lewis acidity of a water ligand bound to a dimanganese(II,II) site over that bound to a single Mn(II) ion can be estimated by using a thermodynamic cycle from published data. The pK_a for proton ionization from a water molecule bound between two aquamanganese(II) ions, the reverse of eq 2d, can be estimated using the known binding equilibria given in eqs 2a and 2b,[49] the water ionization constant, eq 2c, and an electrostatic approximation.[22] In these reactions waters of hydration are not denoted unless they are released as a consequence of the indicated reactions. All reactions refer to the fully aquated ions. The appropriate units for each equilibrium constant are indicated in parentheses.

$$OH^- + Mn^{2+} \rightleftharpoons Mn(OH)^+ + H_2O \qquad \log K = 3.4(M^{-1}) \qquad (2a)$$

$$OH^- + 2\,Mn^{2+} \rightleftharpoons [Mn^{OH}Mn]^{3+} \qquad \log K = 3.4(M^{-2}) \qquad (2b)$$

$$H_2O \rightleftharpoons H^+ + OH^- \qquad \log K_w = -14(M^2) \qquad (2c)$$

$$[Mn^{OH_2}Mn]^{4+} \rightleftharpoons [Mn^{OH}Mn]^{3+} + H^+ \qquad \log K = ? \qquad (2d)$$

$$H_2O + 2\,Mn^{2+} \rightleftharpoons [Mn^{OH_2}Mn]^{4+} \qquad \log K = ? \qquad (2e)$$

$$Mn(OH)^+ + Mn^{2+} \rightleftharpoons [Mn^{OH}Mn]^{3+} \qquad \log K = 0\,(M^{-1}) \qquad (2f)$$

The equilibrium constant for the proton ionization in eq 2d can be determined from the other equilibria if the association constant is known for formation of the μ-aqua-bridged dimer in eq 2e. Unfortunately, this is not available in the literature. However, ionization of a proton from aquamanganese(II) has a pK_a of 10.6 (eq 2a + eq 2c). Hence, relative to free

Table III.A.1. Both the Catalase and Arginase Activities of Liver Arginase Require the Dimanganese(II,II) Center [Sossong et al. (1996); Cavallie et al. (1994)]

		L-arginine hydrolysis			
mutant	Mn/trimer	K_M (mM)	k_{cat} (rel), %	peroxide dismutation O_2 rate, %	proposed function
wild-type	6	1.4	100	100	
HIS101ASN	3	2.2	0.17	0.5	Mn ligand
HIS126ASN	3	0.8	0.001	2.7	Mn ligand
HIS141ASN	6	9	10	100	cat. base

water which has $pK_w = 14$, the effect of replacing a proton on water by a Mn(II) ion is worth 3.4 pK units in free energy of stabilization. Assuming the second Mn(II) ion produces the same degree of stabilization as the first, then the pK_a for eq 2d should be $10.6 - 3.4 = 7.2$. Because the bonding in aqua Mn(II) and the hydroxide hydrolysis product is essentially ionic, this electrostatic approximation has been found to accurately predict the spin density distribution of binuclear Mn(II) complexes and both the hydration structure and dynamical properties of Mn(II) in water.[50,51]

A second method for estimation of the pK_a is to use the equilibrium constants in eqs 2a and 2b to calculate eq 2f. Comparing eqs 2a and 2f indicates that the binding of Mn(II) to $Mn(OH)^+$ vs OH^- is less favorable by $\Delta \log K = -3.4$. Hence, we can estimate $\log K$ for formation of the aqua dimer in eq 2e to be $-3.4 - 3.4 = -6.8$, which is essentially using an additive electrostatic model. From this number, we get $\log K = -7.2$ for eq 2d as the sum of eqs 2b − 2e + 2c. This model gives the same estimated pK_a for proton ionization as the previous model, while also utilizing the independently determined equilibrium in eq 2b to estimate the unknown equilibrium in eq 2e. The proton acceptor in this model is water. Other factors such as the nature of the remaining ligands and how they interact with the water ligand will also greatly influence its pK_a in a manner which could yield changes as large as the binuclear effect summarized here.

Comparison to the pK_a for the arginase hydrolysis reaction (7.9−8.0) indicates reasonable correspondence, thus supporting a model in which the role of the binuclear site could be to produce a lower pK_a, i.e., a stronger Lewis acid, than is achievable with a single Mn(II) ion. The lower pK_a would allow formation of a hydroxide anion that could be a candidate for the active nucleophile in the hydrolysis reaction. A hydroxide ion that bridges between the two Mn(II) ions is not expected to be a readily available nucleophile, compared to a terminal hydroxide ligand, even though thermodynamically it is easier to form than a terminal hydroxide ligand. This arises because two of the lone pairs of electrons are tied up in bonding to the Mn(II) ions and thus in a static model would not be available for attack of the substrate. However, the rate-limiting step in substrate hydrolysis under steady-state turnover conditions is relatively slow, about 250 s^{-1}.[45] Hence, if dissociation of a μ-hydroxide from one of the Mn(II) ions were to occur at this rate or faster, it would be converted to an effective nucleophile for hydrolysis. Ligand exchange rates on dimanganese centers have not been reported yet, but the exchange rates for a variety of neutral ligands bound to Mn(II) fall in the range 4×10^5 to 5×10^7.[52] On this basis we predict that bridging hydroxides should be kinetically effective nucleophiles for slow hydrolysis reactions ($<10^3$ s^{-1}).

A terminal hydroxide ligand on a binuclear Mn(II) center also qualifies as a potential nucleophile, but will be a stronger base than a bridging hydroxide and hence found in lower concentration at neutral pH. This may be compensated by the presence of internal bases which serve to deprotonate the water. There is kinetic evidence for a conserved histidine residue, His 141, that is essential for catalysis. This residue has been suggested to function as a general base and is apparently not ligated to either of the Mn ions.[45,46]

2. Catalase Activity of Arginase

Arginase also exhibits a weak catalase activity. The catalytic efficiency (k_{cat}/K_M) of arginase in peroxide dismutation is 10^5-10^6 slower than the bacterial dimanganese catalases, as summarized in Table III.A.2.[22] This lower activity appears to be due either to the inability of peroxide to oxidize arginase above the Mn_2(II,II) oxidation level, or the lack of critical acid/base residues in the active site that are needed for coupled proton exchange with the substrate. A higher reduction potential for arginase vs Mn catalase would be expected if fewer carboxylates (more neutral ligands, i.e., histidine or water) coordinate to the Mn_2 center. Inhibitors of the arginase activity (L-lysine, N^{ω}-hydroxy-L-arginine) also inhibit the catalase activity of arginase, indicating that the dimanganese site is directly involved in activity. Also, cyanide (HCN/CN^-), a potent inhibitor of heme catalases, is not able to inhibit the catalase activity of arginase.[22] This result is also true for Mn catalase and has been ascribed to the inability of the two Mn(II) ions to move sufficiently far apart to allow linear bridging of CN^- (*ca.* 4.8 Å Mn−Mn distance).

Point mutations of conserved residues in the rat liver enzyme expressed in *E. coli* have shown that mutations His101Asn and His126Asn each lead to loss of 3 Mn/trimer, exactly half of the wild-type level, with concomitant loss of both the arginase and catalase activities (Table III.A.1). Restoration of the hydrolytic reaction occurs in both mutants upon binding of one Cd^{2+} ion to form the heteronuclear MnCd enzyme, while the catalase activity is not restored by binding of Cd^{2+}.[22] Thus both Mn ions are required for the redox function in the catalase reaction. Mutagenesis of the conserved His141 to an Asn residue produces no loss of Mn binding and no change in the relative catalase activity. Thus His141 plays no dominant role in Mn binding. It also does not influence the relatively slow kinetics of the rate-limiting step of the dismutation reaction. Since Asn is capable of replacing His as a proton transfer site (albeit with a higher proton affinity) this result does not exclude a role for His in proton transfer steps in the catalase reaction.

So what controls the redox vs hydrolytic activity of the binuclear site of arginase? The evidence from the His mutants in Table III.A.1, showing that both Mn ions are required for the catalase reaction, suggests a ping-pong mechanism involving Mn_2(II,II) ↔ Mn_2(III,III) redox cycling, directly analogous to the Mn catalase enzymes. Studies on dimanganese model

Table III.A.2. Steady-State Kinetic Parameters for the Dismutation of Hydrogen Peroxide by Mn Catalases and Rat Liver Arginase

Mn_2(II,II) protein	k_{cat} (s^{-1})	K_m (mM)	k_{cat}/K_M (M^{-1} s^{-1})	ref
T. thermophilus	2.6×10^5	83 ± 8	3.1×10^6	55
L. plantarum	2.0×10^5	350	5.7×10^5	35
T. album	2.6×10^4	15	1.7×10^6	114
Liver Arginase	30	2,750 ± 250	11	22

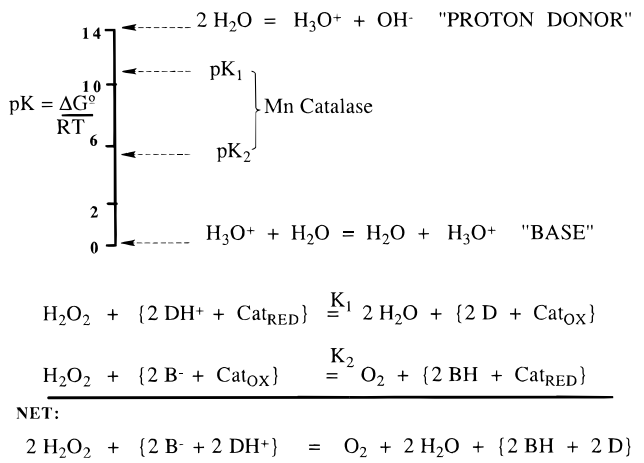

Figure III.A.3. By coupling the dismutation reaction to H^+ donors and acceptors other than water the free energy change ($\Delta G°$) can be increased and used to accelerate catalysis. DH and B^- are a proton donor and acceptor, respectively.

complexes also support a shared redox function for the two Mn ions.[32] Distinct functions for the two metal ions, such as redox cycling at one Mn center between Mn(II) and Mn(IV) and acid/base chemistry promoted at the second Mn(II) site, appear to be excluded. Why is there a 10^5-10^6 fold lower catalytic efficiency, k_{cat}/K_M, for the catalase reaction by arginase? The 4 times weaker Mn−Mn superexchange energy in Mn(II,II)arginase vs Mn(II,II) catalase indicates a different bridging ligand structure which may contribute to the large difference in catalase rates. Three candidates for the different reactivities are the higher reduction potential predicted for arginase vs Mn catalase, a lower binding affinity for peroxide (H_2O_2 or HO_2^-) at the active site, or the lack of proton donors and acceptors in the active site needed for the dismutation reaction. A kinetic limitation based on lower substrate accessibility to open- or solvent-labile coordination sites on Mn is not a likely explanation, considering the enzyme's accessibility to a variety of inhibitor molecules in the active site. Moreover, ^{1}H ENDOR studies of the Mn_2 site of arginase indicate the presence of labile water protons that exchange in ^2H_2O, and thus solvent exchange is facile.[53]

In the first case, if oxidation of the binuclear Mn site in arginase were rate limiting for catalase activity we would predict a slower rate vs Mn catalase by 10^7-fold, assuming an endothermic reaction with a 0.5 eV greater reduction potential and using Eyring rate theory. The ligand field contribution to the Mn(III) reduction potential can be partitioned into two components: that arising from ionizable residues (pH dependent) and that arising from residues which do not participate in pH dependent equilibria. The pH-dependent part of the reduction potential can be determined from known equilibria in many cases, as summarized in Figure III.A.3. The reduction potentials of Mn catalase and arginase are not known at present, but the pH dependence of the catalase activity is known. For the half-reaction involving reduction of arginase by peroxide, proton transfer from the substrate to a base (B^- in Figure III.A.3) having acid dissociation constant equal to pK_2 will contribute to the thermodynamic driving force of the half-reaction by an amount equal to eq 3.[20,54]

$$\Delta\Delta G_2 = RT \ln [1 + 10^{(pH-pK_2)}] \qquad (3)$$

This free energy shift is relative to the potential at low pH where the base BH is fully protonated and hence unavailable for coupling to the catalase reaction, i.e. when water is the only proton acceptor. Equation 3 predicts that if arginase has no proton acceptor other than water it will have a smaller thermodynamic driving force than the case of a proton acceptor with $pK_2 = 5.5$, i.e. as found in Mn catalase. The lower proton affinity would reduce the free energy of stabilization by 2.0 kcal/mol in arginase vs Mn catalase. If this thermodynamic barrier were to contribute to the kinetic barrier for the rate-determining step in the catalase reaction of arginase, we could expect a slower rate by a factor of $k/k_{max} = 0.04$, using Eyring rate theory. This 25-fold reduction could contribute to the slower catalase rate observed with arginase, but is insufficient to account for the observed 10^5-10^6 difference. Hence, differences in the identities of the proton transfer groups in the active sites of arginase vs catalase are unlikely to be solely responsible for the large rate difference.

This leaves as a possible source of the large difference in catalase activities a redox potential difference or a difference in peroxide binding affinity. The electrochemical potentials of Mn catalase and arginase have not been determined and so their contribution to a thermodynamic barrier could not be estimated. On the other hand, there is an 8−200-fold larger Michaelis constant (K_M) for hydrogen peroxide disproportionation in arginase (2.75 M) than for either *T. thermophilus* Mn catalase (0.083 M), *L. plantarum* Mn catalase (0.35 M), or *T. album* Mn catalase (0.015 M).[55] This lower affinity for peroxide binding to arginase also contributes to the 10^5-10^6-fold overall lower catalytic efficiency.

B. Manganese Catalases

Catalases protect organisms from oxidative damage by serving as surveillance enzymes to scavenge the appreciable levels of hydrogen peroxide produced during O_2 metabolism in cells. As much as 10% of the O_2 consumed in cellular respiration may be reduced to hydrogen peroxide. Peroxide is readily reduced to hydroxyl radicals and hydroxide ions by a variety of one-electron reductants commonly found in cells. The resulting hydroxyl radical is an indiscriminate potent oxidant which is capable of oxidizing all cellular components it comes in contact with. In this capacity catalases provide the first line of defense against oxidative stress and associated degenerative diseases, including possibly forestalling the onset of cancer and aging.[56,57]

Mn catalases have been characterized from a few bacteria. The most extensively studied enzymes come from the extremely thermophillic *Thermus thermophilus* (*Tt*) and the lactate-requiring *Lactobacillus plantarum (Lp)*.[58,59] The enzyme exists as a hexamer of six equivalent subunits, each with a molecular mass of 35 kDa. A 3 Å X-ray structure of *Tt* Mn catalase has revealed a four-helix bundle motif as the major secondary and tertiary protein folding

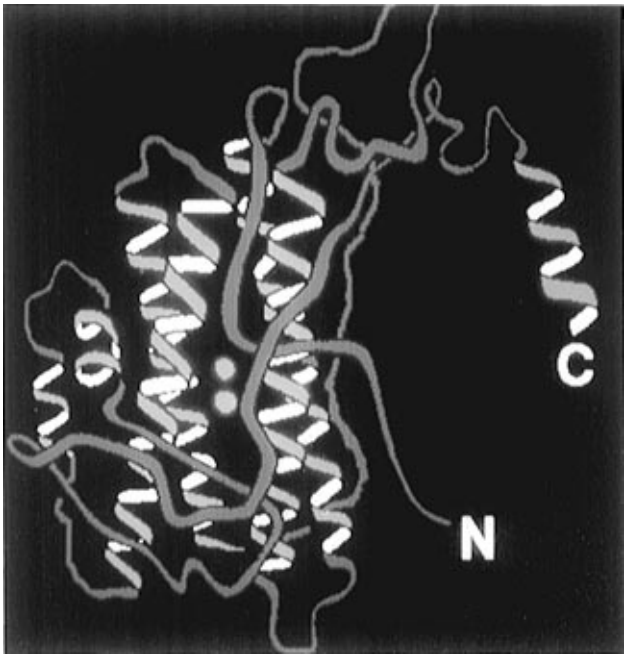

Figure III.B.1. *T. thermophilus* manganese catalase 3.0 Å X-ray structure. Ribbon diagram of α-carbon tracing. From Barynin et al. (1986) with permission.

elements in each subunit, as depicted in Figure III.B.1.[60,61] This characteristic motif is found in a diverse family of proteins comprised of hemerythrin, apoferritin, cytochrome *c′* and *b*562, methane monooxygenase, ruberythrin, TMV coat protein, and *E. coli* ribonucleotide reductase.[8,25,62] The metal-binding site in the first four examples and presumably manganese catalase is comprised of side chains derived from several α-helices and lies nestled within the interior surfaces of the helices. Each subunit contains a pair of Mn ions separated by 3.6 Å. The amino acid residues that ligate the Mn ions have not been identified yet by X-ray diffraction. A 2.2 Å data set has been available since 1991; however, only recently has the protein sequence been determined (D. Ash and V. Barynin, private communication). A refined atomic map of the protein is said to be nearing completion (V. Barynin, private communication).

There are four oxidation states of Mn catalase that have been characterized, symbolized in terms of the formal Mn oxidation states as (II,II), (II,IIII), (III,III), and (III,IV). Only the (II,II) and (III,III) states have been shown to catalyze the dismutation of hydrogen peroxide at extremely high rates.

EPR spectroscopy first revealed that Mn catalase contains a binuclear Mn center, and this technique has been applied extensively to characterize the electronic structure of three of the four known oxidation states.[63−65] EPR reveals that reduced Mn(II,II) catalase contains a pair of antiferromagnetically coupled Mn(II) ions. Two excited-state EPR signals (triplet and quintet spin states) can be observed above a diamagnetic ground singlet state in both the *Tt* and *Lp* enzymes.[31,66] These have temperature dependences that fit well the predicted Boltzmann expression for a pair of Mn(II) ions coupled by isotropic Heisenberg spin exchange ($-2JS_1 \cdot S_2$). In the case of the reduced *T. thermophilus* enzyme the spin exchange energy for the phosphate derivative is weak (-5.6 cm^{-1}), and qualitative estimates for the other anion bound derivatives indicates a range of values (-5 to -15 cm^{-1}).[31] Comparison of the Heisenberg exchange interaction constants to more than 30 dimanganese(II,II) complexes suggests a possible bridging structure of (μ-OH)(μ-carboxylate)$_{1-2}$ for the unliganded form of MnCat(II,II) at neutral pH.[31] Table III.B.1 lists several physicochemical properties of Mn catalase-(II,II) from both *T. thermophilus* and *L. plantarum*.

The enzyme isolated from *L. plantarum* exhibits a Heisenberg exchange coupling of -5.2 cm^{-1} for the fluoride derivative and -20 cm^{-1} for the unliganded derivative at neutral pH.[66] Both enzymes take up one proton from solution per anion binding event, which may indicate either proton uptake or release of OH$^-$.[66,67] On the basis of these data the core structure of the unliganded form of the *Lp* enzyme has been proposed to contain a di-μ-hydroxo bridge which is replaced by di-μ-fluoro bridges and release of 2 OH$^-$ upon binding with fluoride.[66] A single μ-hydroxo bridge and a single μ-bridging anion site have been proposed for the *Tt* enzyme,[37] along with one or two μ-carboxylates (see below). Recent L-edge X-ray absorption spectroscopy measurements indicate that the octahedral component of the ligand field, which splits the valence 3d orbitals of reduced *Lp* Mn catalase, is about 1.1 eV, a value typical of O or N ligands with a coordination number of 6.[68]

Table III.B.1. Properties of the Dimanganese(II,II) Center in Arginase and Catalase[a,b]

Mn(II) Mn(II) pair in	r(Mn−Mn) (Å)	D_2 (ZFS) (cm^{-1})	J (cm^{-1})	IC50 (mM)
MnCat(aquo), *Tt*	≥3.70	<|0.025|		none
MnCat(phosphate), *Tt*	3.59	−0.051	−5.6 ± 0.1	nm
	3.63	−0.040		
MnCat(acetate), *Tt*	3.51	−0.071	nd	23
MnCat(chloride), *Tt*	3.51	−0.071	nd	0.20
MnCat(fluoride), *Tt*	3.31	−0.120	nd	0.25
MnCat(cyanide), *Tt*	3.63−3.70	−0.040 to −0.025	nd	≫25 mM
MnCat(aquo), *Lp*	nd	nd	−20	none
MnCat(fluoride), *Lp*	3.4	−0.094	−5.2	0.012 $K_{D,1}$
		(dipole + zfs)		0.14 $K_{D,2}$
arginase(+borate)	3.50	-0.073	−2.0 ± 0.5	
arginase(−borate)	3.57	-0.056		
	3.52	-0.069		
	3.36	-0.105		

[a] r(Mn−Mn) intermanganese sepatation; D_2 dipolar zero-field splitting from quintet state; J intermanganese Heisenberg exchange interaction for $H = -2JS_1 \cdot S_2$; IC50 is the concentration of anion that induces 50% inhibition of the catalase activity at pH 6.3, while $K_{D,1}$ and $K_{D,2}$ refer to binding constants not activity. [b] Data for arginase and *T. thermophilus* Mn Catalase from refs 31 and 37; for *L. plantarum* Mn Catalase from ref 66.

In both the triplet and quintet states of Mn(II,II) catalase the EPR signal exhibits zero-field splitting (ZFS) that has its major source from the magnetic dipole−dipole interaction between the Mn(II) ions. Because of the spherically symmetric spin distribution of the half-filled 3d shell of Mn(II), a linear correlation is observed between the ZFS of the quintet state (D_2) and the crystallographically determined Mn−Mn distance for several dimanganese pairs for which both data sets are available.[31] Using this correlation the Mn−Mn distance has been determined for a number of the inhibited complexes of *Tt* Mn(II,II)Cat, and these are listed in Table III.B.1. The distance between the Mn(II) varies between 3.31 Å (F^-) and ∼3.7 Å (unliganded, pH 7) for a variety of anions in a systematic way with size of the anion, consistent with binding to both Mn ions at a μ-bridging position.[37] The unliganded "aquo" form of Mn(II,II)Catalase has the longest separation of all complexes at ≥3.7 Å. This range of distances is suggestive of one or two μ-carboxylate bridges from the protein spanning the Mn ions.

Only anions possessing two or more lone pairs of electrons per atom exhibit evidence of binding to the bridging site in the (II,II) oxidation state and of simultaneously inhibiting the catalase activity. By contrast, cyanide exhibits a special behavior in that it does not inhibit catalase activity of the unliganded enzyme (Table III.B.1) and actually *reverses* inhibition caused by the inhibiting class of anions. Reactivation is independent of pH between 6.5 and 8.5, indicating that HCN is the active form involved in reactivation of catalase activity. Cyanide appears to bind to a terminal (nonbridging) site on one or both Mn(II) ions, as seen by the increase in the intermanganese distance to the aquo limit. This terminal ligation preference has been ascribed to the linear sp-hybridized electronic structure of cyanide, which having only a single nonbonding pair of electrons per atom cannot bind between two Mn ions, unless these can be separated by 4.8 Å. Inhibition of catalase activity by anions seems to be governed by the lack of kinetic lability at the bridging site, as evidenced by the slow kinetics of inhibition by anions and the slow kinetics of reactivation upon removal of anions. Apparently bridging anions exchange more slowly than terminally ligated anions and thus inhibit effectively. The stimulation of activity by cyanide suggests that bridging anions can be displaced to a labile terminal coordination site on one Mn ion. The two sites are in equilibrium with one another, thereby allowing anions to exchange sites. Rapid dissociation of anions that bind to the terminal site on one of the Mn ions occurs in competition with substrate binding thereby reversing inhibition. These various data (metrical, Heisenberg exchange and correlation with activity) have led to the proposed core structure of the active and inhibited forms of MnCat given in Scheme III.B.1.[37]

The Mn ions in catalases can be oxidized, yielding three higher oxidation states: (II,III), (III,III), and (III,IV).[34,64,65] Extended X-ray absorption spectroscopy (EXAFS) reveals that the Mn−Mn distance shortens appreciably to 2.7 Å in the catalytically inactive (III,IV) oxidation state, a feature attributed to formation of a di-μ-oxo bridge.[69] A di-μ-oxo bridge

Scheme III.B.1. Core Structure of Mn(II,II)Cat and Anion (X^-) Binding Equilibria. From Shank et al. (1996).

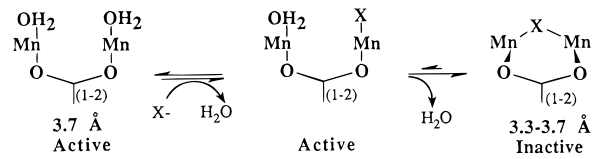

has also been implicated on the basis of EPR temperature dependence[8] and electronic spectroscopy studies.[70] Electron−nuclear double resonance (ENDOR) and electron spin−echo envelope (ESEEM) studies of Mn(III,IV)Cat have revealed that most of the protein ligands lack atoms having magnetic moments, i.e., lack protons in the first three coordination shells, and thus are comprised predominantly of carboxylate residues (Asp, Glu) or oxygens.[71] A single N-donor ligand is also detectable by ESEEM (terminal histidine(?)[72] or possibly a μ-bridging lysine residue(?)[73]). The coordination number of the Mn(III) ion is 6 and the electronic configuration of the Mn(III) has the usual Jahn−Teller distorted ground state, $(d_\pi)^3(d_{z^2})^1$.[51] A single labile water molecule also binds in the second shell of ligands and could be H-bonded to the μ-oxo bridges.[71]

Both heme and Mn type catalases dismute H_2O_2 at exceedingly high rates approaching that of a diffusion limited reaction. The physiological activity of Mn catalase is found exclusively in the (II,II) and (III,III) oxidation states, and a cyclic ping-pong mechanism is believed to interconvert the two oxidation states.[8,35] Previous steady-state kinetic studies on *Tt* catalase indicate a rate-limiting step that is first order in enzyme and peroxide concentrations, involving interconversion between reduced Mn(II,II)Cat and oxidized Mn(III,III)Cat.[67,74] These oxidation states are also found for the active forms of Mn catalase isolated from *Lp* based on X-ray absorption edge studies.[75] Saturation kinetics are observed with respect to substrate, corresponding to a Michaelis−Menten rate law for all three known sources of the enzyme, as summarized in Table III.A.2. The Michaelis constants (K_M) differ by 20-fold, while the catalytic efficiencies (k_{cat}/K_M) exhibit only a 5-fold variation with species. Protons from solution are not required in the rate-limiting step between pH 6 and 10. However, ionizable protein residues with pK_a 5.5 and 10.5 are essential internal acid/base catalysts in the *Tt* enzyme.[67,76]

The (III,III) oxidation state of Mn catalase is the predominant form of the enzyme under aerobic conditions of isolation. It lacks an EPR signal, but exhibits characteristic visible and near ultraviolet absorption bands (Table III.B.2) that were tentatively assigned to charge-transfer bands of type oxo → Mn(III) and carboxylato(O) → Mn(III) and weaker Mn(III) ligand field transitions on the basis of comparison to μ-oxo-di-μ-carboxylato-dimanganese(III,III) complexes and their resonance Raman excitation profiles.[77] The electronic spectrum differs from that observed in the (III,IV) oxidation state (Table III.B.2), which is blue shifted and has higher absorptivity. The spectrum of this oxidation state has been interpreted on the basis of variable-temperature magnetic circular dichroism, ligand field calculations and reso-

Table III.B.2. Electronic Absorption by Mn(III,III) and Mn(III,IV) Catalase[a]

λ_{max}, nm absorptivity,[b] M^{-1} cm^{-1}	*T. thermophilus*	*L. plantarum*
(III,III)	280 (32,000)	
	395 sh (340)	380 sh (290)
	475 (300)	470 (270)
	500 (300)	485 sh (260)
	600−800 tail (60 at 700)	680 (70)
(III,IV)		360 sh (1,680)
	410 (1,650)	440 (928)
	560 (320)	630 (320)

[a] Data for *L. plantarum* Mn(III,III) catalase is from ref 59; *L. plantarum* Mn(III,IV) catalase, from ref 70; *T. thermophilus* Mn(III,III) and Mn(III,IV) catalase, from ref 74. [b] Absorptivity is per mole of dimanganese subunits.

Scheme III.B.2. A Possible Mechanism of Peroxide Dismutation by Dimanganese Catalases

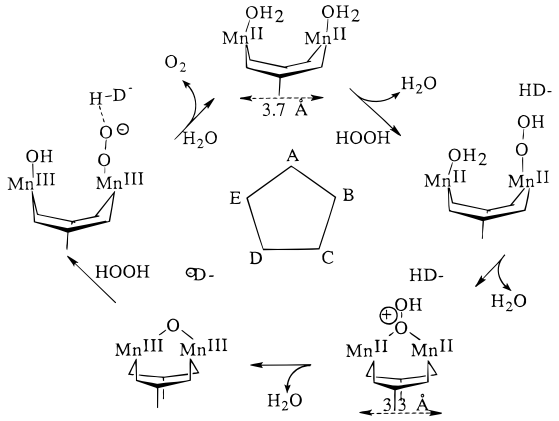

nance Raman studies of model complexes, which support a core structure having the di-μ-oxo-mono-μ-carboxylato bridge.[70] The presence of the di-μ-oxo core is in good agreement with the interpretation of Mn EXAFS studies and simulations of the EPR spectrum and its temperature dependence.[51,69]

An atomic level mechanism for catalysis by Mn catalases can be proposed on the basis of these data and is given in Scheme III.B.2. In the first step of the reaction (A → B) substrate binds directly to a terminal site on Mn(II) by displacement of a water ligand. This is proposed on the basis of the aforementioned anion binding studies, which suggested that substrate exchange occurs initially at a terminal site (as was found in studies with cyanide). An internal protein residue is imagined to function as proton acceptor for ionization of hydrogen peroxide and later to deliver the proton to form the product water. This could be the catalytically important base with pK_a ~5.5. Activation of peroxide for reduction to the oxide level is imagined to occur following a critical step in which the terminally ligated substrate (B) swings over to form a μ-η^2-peroxide (C). This binding mode is proposed on the basis of the anion binding studies demonstrating that anions like F^-, Cl^-, etc. prefer to bind in the bridging site. Reduction of substrate to water and μ-oxo at this site (C → D) should be facilitated by a decrease in the intermanganese distance from ~3.7 to 3.3 Å, as is found upon anion binding to the (II,II) oxidation state (i.e., Scheme III.B.1). The mechanism of the remaining steps is less clear, as there is very little information at present on the (III,III) oxidation state. However, the μ-oxo bridge is known to be readily exchangeable with H_2O^{18} upon protonation in mono-μ-oxo-dimanganese model complexes.[77−79] On this basis, protonation of μ-oxo and cleavage of the bridge is proposed to occur upon binding of the second substrate molecule to a terminal Mn(III) site (D → E). Subsequent intramolecular two-electron transfer from hydroperoxide to reduce both Mn(III) ions, coupled to proton transfer to the catalytic base, would complete the cycle by generating O_2 and the reduced aquo complex (E → A).

In this mechanism, the extraction of free energy to aid in driving the reaction can be imagined to occur in two stages. First, coupling of proton transfer from the first substrate molecule to a low-affinity protein site which will eventually form one of the two product water molecules, species D^- in steps A → B → C → D. Second, coupling of proton transfer from the second substrate molecule to a high-affinity protein site (also species D^-) which will eventually form the second product water molecule (D → E → A). For simplicity in drawing, the same symbol is used in Scheme III.B.2 to designate both the proton donor and acceptor in this mechanism (species DH/D^-). This gives the impression that no free energy change associated with proton transfer can couple to the product formation. However, if two different acid/base groups are involved in this process, as summarized previously in Figure III.A.3 ($DH + B^- \rightarrow D^- + BH$), then their difference in acidites could be the source of protonic free energy. Even if the proton donor and acceptor in Scheme III.B.2 are the same group, they may have different pK_a values arising from the influence of different charge distributions in the active site in the steps linked to proton transfer.

A recent alternative mechanism has been proposed in which interconversion of $Mn_2^{II}(\mu\text{-OH})_2$ and $Mn_2^{III}(\mu\text{-O})_2$ core structures forms the basis of the catalytic mechanism.[66]

C. Hydrolysis of Phosphodiester Bonds in Polynucleic Acids by Bimetallic Enzymes

1. Exonuclease of DNA Polymerase and RNase H

Replication of and infection by the human immunodeficiency virus type 1 (HIV-1 virus) requires DNA synthesis by reverse transcriptase (RT), a retrovirus-encoded RNA-dependent DNA polymerase. HIV-1-RT is a multifunctional enzyme required not only for the synthesis of the double-stranded proviral DNA from the single-stranded retroviral RNA genome but also for cleavage of the retroviral RNA polymer in the form of a hybrid DNA−RNA intermediate. This latter activity, called ribonuclease H or RNase H activity, allows transcription of the RNA fragments to proceed. These two functions are localized in separate domains of the enzyme. The enzyme requires either Mg^{2+} or Mn^{2+} for activity. HIV-1 RT has two subunits of 66 and 51 kDa, both of which are needed for an active heterodimer. The 66 kDa subunit contains the DNA polymerase and RNase H domains, whereas the 51 kDa subunit, obtained by proteolytic digestion of the larger subunit, has only the DNA synthetic activity. The remaining 15 kDa carboxyl terminus is inactive as an RNase H but can

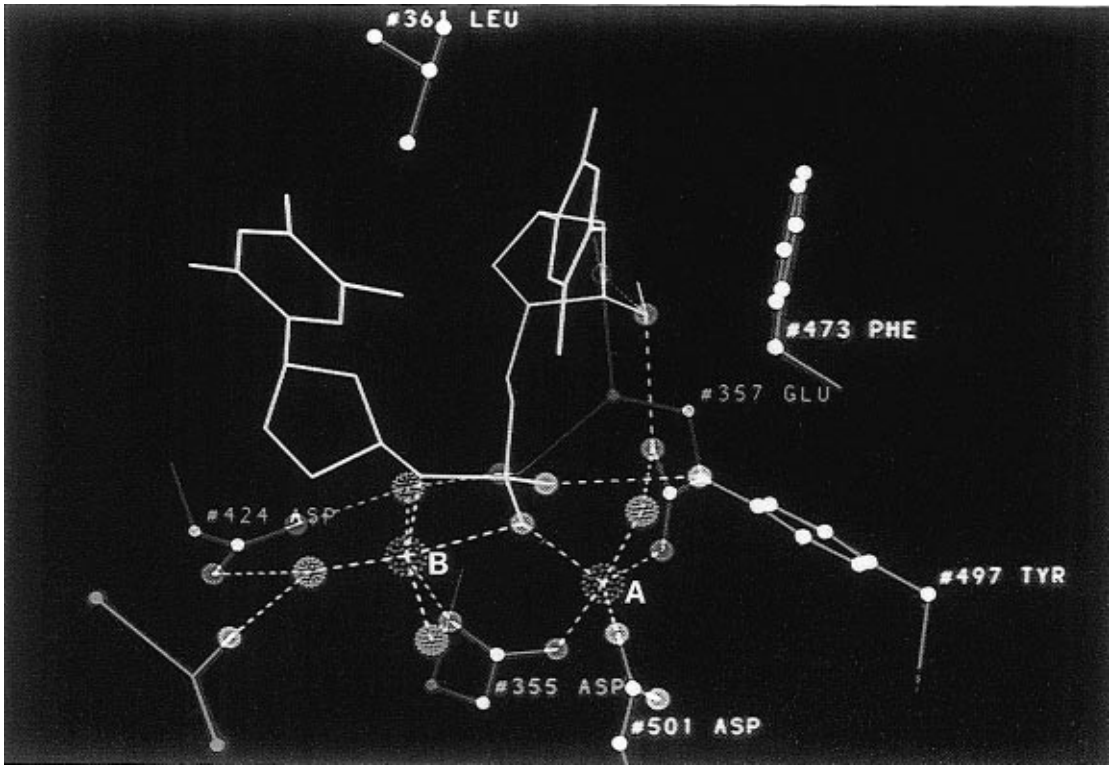

Figure III.C.1. Overview of the 3′−5′ exonuclease active site showing a bound deoxydinucleotide. The positions of the sugar and base of the penultimate nucleotide are determined from the tetranucleotide complex, while the 3′ terminal nucleotide and the remaining coordinates are from the dTMP complex. The side chains of residues interacting with the metal ions and dTMP are shown. The two binding sites for divalent metal ions are labeled A and B and are 3.0 Å apart. Metal ligand distances are between 1.9 and 2.2 Å and H bond distances are between 2.7 and 3.0 Å. From Beese and Steitz (1991) with permission.

be fully reactivated by addition of the 51 kDa polymerase domain, confirming the functional interdependence of the two subunits in the native enzyme. The steps in the life cycle of the virus which RT catalyzes include: (1) RNA-dependent DNA polymerase; (2) RNA hydrolysis; and (3) DNA-dependent polymerase.

The RNase H domain of RT, short-hand for ribonuclease H or more completely RNA−DNA hybrid ribonucleotide hydrolase (EC 3.1.4.34), breaks the phosphodiester bond by hydrolysis of RNA found specifically in RNA−DNA hybrids.[80] An X-ray diffraction structure of the 15 kDa RNase H subdomain of HIV-1 RT has been solved to 2.4 Å resolution and found to exhibit an overall 3-dimensional structure similar to the *E. coli* RNase H, but with unique structural features which are believed to be important to its distinct RNA substrate specificity.[81] In both enzymes, and additionally in the 3′−5′ exonuclease domain of DNA polymerase I, two Mn^{2+} ions have been located in the map, and these have been suggested to be the metal ions required for their catalytic activities. This connection is often obscured in nucleic acids, owing to the many structural metal ions associated with these polyanionic polymers. The polymerase domains of both enzymes also contain a metal-requiring center, not to be confused with the nuclease site. In the case of both HIV-1-RT (RNase H subdomain) and DNA polymerase I (exonuclease subdomain), binuclear metal sites are found in their structures. Despite significant protein-folding differences, four conserved carboxylate residues serve to bind two Mn^{2+} ions. The Mn^{2+} ions are separated by 4 Å by a μ-1,3-bridging carboxylate. The two active-site structures can be superimposed. The structure of the exonuclease domain of DNA polymerase I complexed to a deoxynucleoside monophosphate, dTMP, is depicted in Figure III.C.1.[23] It is clear in the latter structure that the two metal ions bind additionally to one of the oxyanions of the 5′ phosphate of dTMP. One metal ion (A) ligates a water (or hydroxide), while the other metal ion (B) ligates the second oxyanion of dTMP.

On the basis of this structure, Steitz and co-workers have proposed an atomic model for how both metal ions of exonucleases may act to catalyze hydrolysis of polynucleic acids.[23] Figure III.C.2 depicts the proposed transition state in their model. Metal A and its monodentate carboxylate ligand, Glu357, serve to ionize a bound water ligand, forming the hydroxide nucleophile and orienting it for in-line attack at the trigonal face of the phosphate that lies opposite to the departing 3′ hydroxyl of the phosphodiester bond. Metal ion B orients the reactive trigonal face of the tetrahedral phosphate directly at the nucleophilic hydroxide, through coordination to two phosphate oxygen atoms as seen in the structure. It also stabilizes the anionic charge on the 3′ hydroxyl of the cleaved product to which it is directly ligated. This mechanism correctly accounts for the inversion of stereochemistry at the phosphate center by formation of the trigonal−bipyramidal phosphate diester in the transition state. Warshel and co-workers have conducted a theoretical analysis of this mechanism and find good evidence to support its general validity.[24]

The binuclear center appears to play a special role in stabilizing the formation of the trigonal-bipyra-

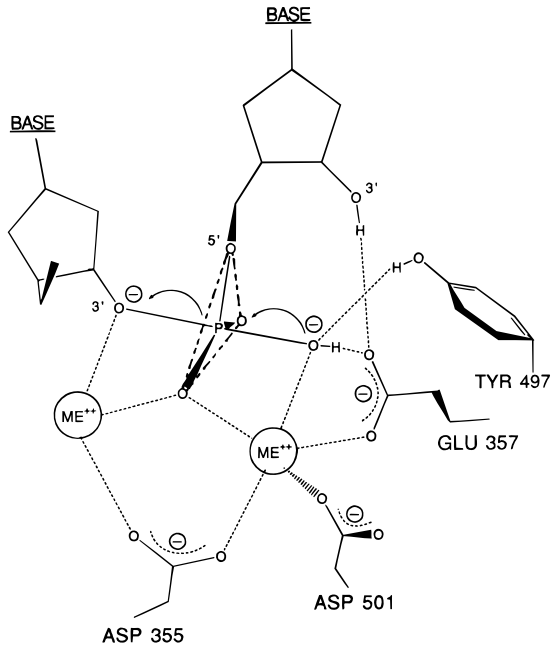

Figure III.C.2. The proposed transition state of the two metal ion enzymatic mechanism for the 3′−5′ exonuclease reaction. Metal ion A on the right is proposed to facilitate the formation of an attacking hydroxide ion whose lone pair electrons are oriented toward the phosphorus by interactions with the metal ion, Tyr497 and Glu357. Metal ion B is hypothesized to facilitate the leaving of the 3′ hydroxyl group and stabilization of the 90° O−P−O bond angle between the apical and equatorial oxygen atoms. From Beese and Steitz (1991) with permission.

midal transition state through the symmetric coordination of the incoming and departing anionic fragments—the "balanced see-saw potential". This feature cannot be readily duplicated in enzymes not possessing binuclear sites. The Lewis acidity of the binuclear site could also be enhanced over that of a monometallic site, by as much as a factor of 3.5 pK units in the case of aqua Mn^{2+} ions, as described above. This electrostatic effect serves to lower the pK_a of the water nucleophile, thereby increasing its concentration at physiological pH.

The similarities in geometrical arrangement of the three conserved carboxylate ligands and the binding of $UO_2F_5^{3-}$ to the active site in one of the heavy atom derivatives of the RNase H domain of HIV-1 RT, has led to the suggestion that it could share a common mechanism of phosphodiester bond hydrolysis as proposed for the 3′−5′ exonuclease of DNA polymerase I.[80,82]

Not all studies support the double metal ion mechanism. Steady-state kinetic studies of the *E. coli* RNase H activity using a synthetic RNA−DNA hybrid as substrate have found a molecularity of one for Mg^{2+} ion in catalyzing the rate-limiting step under steady-state conditions.[83] It is not clear from these data if the binding of Mg^{2+} ion is associated with one or more sites on the enzyme or the substrate or both. An extremely narrow range of Mg^{2+} concentrations could be explored, owing to the onset of substrate inhibition as the Mg^{2+} concentration increases. These kinetic data do not preclude the involvement of a second metal ion in catalysis. In support of the single metal ion hypothesis, an X-ray structure of *E. coli* RNase H has found only a single metal ion coordinated to the protein.[84] However, metal-binding studies were not conducted. The binding of a second metal ion is presumed to be weaker and may not be structurally detectable in the absence of substrate.[85]

2. Ribozymes: Endonuclease Activity of Self-Splicing Catalytic RNAs

Ribozymes are relatively short sections within RNA polymers that function as enzymes to catalyze the cleavage of RNA, so-called self-splicing endonuclease activity. They are found embedded within the intervening sequence regions of various RNAs.[86] The cleavage reaction clearly requires metal ions and may involve two metal ions with distinct functions (Mg^{2+} or Mn^{2+} are equally effective). However, it is not yet clear what are their specific functions in catalysis nor if these form a binuclear center. The "hammerhead" ribozyme is a catalytic RNA which forms a structural motif present in the RNA genome of several plant pathogens. It is believed that the self-splicing cleavage activity is essential for replication of the virus.[87] The recent crystal structures of two inhibitor complexes of hammerhead ribozymes offer hope that all of the catalytic metal ion(s) may eventually become detectable crystallographically.[88,89] The crystal structures did not unambiguously identify the associated Mg^{2+} ion(s), and indirect methods were used to place one hydrated Mg^{2+} ion in the active site.[89] Scott et al. have proposed a single metal ion mechanism based on these structural data. A second more labile site has not been proven (or disproven).

The catalytic ribozyme of *Tetrahymena thermophilia* has been extensively studied by kinetic methods. The rate-limiting step in cleavage is believed to involve attack by a hydroxide ion bound to a divalent metal ion based on two compelling lines of evidence: (1) Although there is no kinetic isotope effect (and hence no proton transfer in the rate-limiting step), the rate slows by 4.4-fold in D_2O vs H_2O, as expected for an equilibrium deuterium isotope effect originating from the 4.5-fold lower concentration of OD^- vs OH^- at the pH of the reaction;[90] (2) the rate accelerates with increasing pH with the same slope for a variety of divalent metal ions, while saturating at different pHs that correlate roughly with the pK_a of the metal ion.[91,92] This step is depicted in Figure III.C.3 where the reaction starts by abstraction of a proton from the 2′ hydroxyl of the substrate RNA molecule by the metal hydroxide base to form the metal 2′-alkoxide. A second divalent metal has been implicated in coordination to the *pro-r* oxyanion of the phosphodiester.[91] This metal has been proposed to stabilize the 5′-oxyanion leaving group that forms in the product. In the second step, the metal 2′-alkoxide attacks the phosphorous to form a 2′,3′-cyclic phosphodiester, with release of the metallo-5′-alkoxide. The symmetric electrical potential, created by a pair of divalent metal ions in the binuclear intermediate, can be anticipated to contribute to a concerted sequence of steps noted above. Such simultaneous nucleophillic attack and product release is a specific example of reaction catalysis mediated by a concerted binuclear metal effect.

A word of caution should be added here. The two metals involved in the proposed transition-state structure given in Figure III.C.3 are brought together

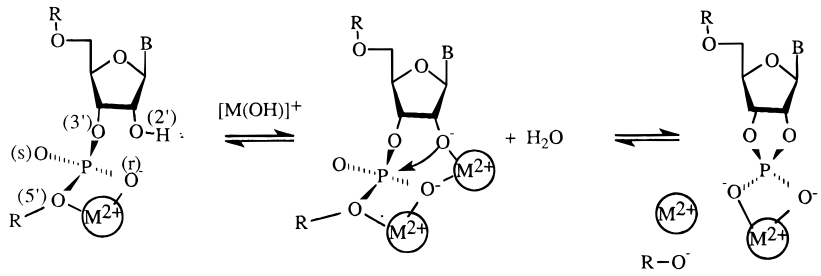

Figure III.C.3. Mechanism of the double metal ion catalysis of RNA substrate hydrolysis by the "hammerhead" ribozyme oftetrahymena thermophilia. Adapted from Sawata, et al (1995) with permission.

by the availability of metal ion coordination sites on the substrate RNA. The metal ions should exhibit appreciable electrostatic repulsion in the absence of substrate and will certainly change coordination and may not even remain bound to the enzyme. Consequently, the involvement of the binuclear site in the catalytic process is an especially challenging hypothesis to establish.

Piccirilli et al. studied the kinetics of cleavage of a nonphysiological all deoxynucleotide substrate which involves formation of the 3′-hydroxyl cleavage product.[93] Comparison of the rates for the 3′-oxo- vs 3′-thio-bridged substrate revealed a 1000-fold rate enhancement with Mn^{2+} vs Mg^{2+}. This result was interpreted as evidence for the essential role of the divalent ion in stabilizing formation of the 3′-thiolate product in the rate-limiting step of catalysis. Direct coordination of the metal at the 3′-oxo group was proposed.

There is also kinetic evidence discounting the importance of a second metal ion involved in the rate-limiting step of catalysis. A recent kinetic study of the rate of cleavage of a synthetic oligonucleotide substrate containing a 5′-bridging phosphorothioate at the single mandatory ribonucleotide (C_{17}) and deoxyribonucleotides elsewhere, found neither a 5′-thio effect on the rate of cleavage, nor a large difference in rates between Mg^{2+} and Mn^{2+}.[94] This has been interpreted to indicate the involvement of only a single divalent cation in the rate-limiting step of enzymatic turnover and that cleavage of the 5′-leaving group is not the rate-limiting step. However, in a more recent kinetic study employing an all-RNA substrate containing a 5′-bridging phosphorothioate linkage found that the attack by the 2′-oxygen on the phophorous is the rate-limiting step in cleavage only for the substrate containing the 5′-thioester linkage and that cleavage to release the 5′-leaving group is the rate-limiting step for the natural all-RNA substrate.[95] These results enable an alternative interpretation of the results by Kuimelis et al.[94] Because the rate-limiting step is not the departure of the 5′-leaving group for the hybrid oligonucleotide used by Kuimelis et al., one might not expect to observe a 5′-thio effect on the rate of cleavage. Hence, it is not possible to exclude the possibility of a binuclear metal site as the catalytic unit based on these results.

3. Chemical Models for Metal Ion-Catalyzed Dephosphorylation of Nucleoside Triphosphates

The principles proposed above for metal ion catalysis of phosphodiester bond cleavage in polynucleic acids have been rigorously examined in the context of metal ion-catalyzed dephosphorylation of purine

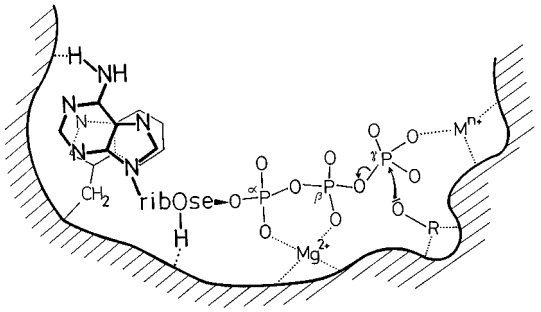

Figure III.C.4. Tentative view of a reactive $Mg(ATP)^{2-}$ complex at an enzyme, the γ-phosphate group being ready for a nucleophilic attack and transfer to R−O which is sitting in a groove of the enzyme. Obviously, the R−O residue could alternatively be bound to M^{n+} and be correctly positioned towards the γ-phosphate group in this way. ATP may be oriented at the enzyme surface by stacking (e.g. with an indole residue) and hydrogen bonding, forcing Mg^{2+} by this orientation, possibly with the help of protein sites, into the α and β positions of the phosphate chain. Obviously, Mg^{2+} and M^{n+} could interchange their positions or other metal ions could substitute for them, and (at least) one of the two metal ions could even be replaced by an ionic interaction (e.g. with an arginyl group) and a reactive intermediate would still result (see text). The release of ADP from the enzyme could in the example shown be initiated by a stronger coordination of the metal ion to the now twofold negatively charged β group leading thus to a release of $Mg(ADP)^-$ from the enzyme surface. (Reprinted from ref 84. Copyright 1984 American Chemical Society.)

and pyrimidine nucleoside triphosphates to form the corresponding nucleoside diphosphate and ortho phosphate.[96] The likely pathways for catalysis by divalent cations involving both a single metal ion and two metal ions have been elucidated. This section does not attempt to offer a comprehensive review of the recent literature on chemical models.

There is firm evidence for distinct roles for two divalent metal ions in these reactions, as summarized in Figure III.C.4. One metal ion is chelated to two oxyanions derived either from the α and β phosphates, or the β and γ phosphates (only the former case is illustrated here). This metal ion stabilizes formation of the additional charge that forms on the β phosphate upon cleavage of the $\beta-\gamma$ bond. The second M^{2+} is monoligated to the terminal phosphate, binds water, and is active only following deprotonation to form the monohydroxo species, $M^{2+}(\gamma\text{-NTP})$-OH. The aqua complex is inactive. Thus, the terminal M^{2+} site serves primarily to promote ionization of the aqua ligand by lowering its pK_a and delivering it to the γ-phosphate as the hydroxide nucleophile. As suggested in Figure III.C.4, the terminal M^{2+} in NTP-dependent enzymes may also serve to weaken the $\beta-\gamma$ P−O−P bond to allow a protein-derived

nucleophile ($R-O^-$) to break this bond by attack at the terminal phosphate.

D. Other Dimanganese Proteins

1. Enolase

Enolase catalyzes the reversible dehydration of 2-phospho-D-glycerate (2-PGA, **4**) to form phosphoenolpyruvate (**6**) in the glycolytic pathway, eq 4.[97] This step creates a highly activated phosphoryl group in **6** that is capable of synthesizing ATP from ADP in the final step of glycolysis.

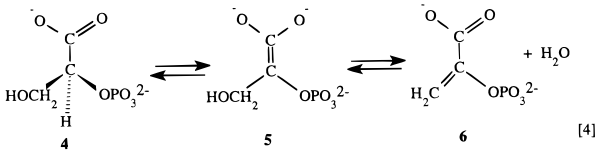

[4]

The reaction in eq 4 is believed to proceed in two steps with formation of a nucleophillic carbanion intermediate, the *aci*-carboxylate **5**. Catalysis of this reaction requires rate acceleration of carbon deprotonation at C-2, where the ionization constant is unfavorable ($pK_a \approx 28-32$). The subsequent step involves release of hydroxide and conversion of the *aci*-carboxylate dianion into carboxylate. The *aci*-carboxylate intermediate must be protected from solvent and dioxygen because it is a strong nucleophile and can decarboxylate. A loop of the protein wraps around the substrate and appears to serve a role in sequestering the intermediate from solvent access.[98] Catalysis of the initial step in this reaction, deprotonation of the carbon acid, is a general feature in several classes of enzymatic reaction types including dehydrations, isomerizations, and racemizations.[99]

The enzyme contains a bimetallic center that is essential for catalysis. Both $(Mg^{2+})_2$ and $(Mn^{2+})_2$ forms of the active enzyme have been characterized spectroscopically.[100] One of the divalent metal ions binds tightly and has been called the "structural" metal site I, while a second metal binds in the presence of substrate or substrate analogs has been called the "catalytic" metal site II. Several high-resolution crystal structures of enolase, primarily from yeast but also from lobster muscle, are available which present atomic models for the holoenzyme and the complexes with substrate and product molecules as well as a substrate analog. A consistent stereochemistry for binding of the substrate analog phosphonoacetohydroxamate to both metal ions of the binuclear center has been established independently by X-ray diffraction of the $(Mg^{2+})_2$ enzyme and by EPR studies of the $(Mn^{2+})_2$ enzyme.[98,100] The binding of 2-PGA to an inactive form of the enzyme containing only a single divalent ion at site I has also revealed its role in coordination of the phosphate group.[101] Most recently the structure of the fully active enzyme with both metal sites occupied and bound to both substrate and product molecules present as a 1:1 equilibrium mixture of 2-PGA and *P*-enol pyruvate has been solved.[102] These independent structural studies have led to three somewhat contrasting views for catalysis to be proposed.[98,101,103]

The most recent mechanistic proposal is based on the structure of the complexes between the $(Mg^{2+})_2$-

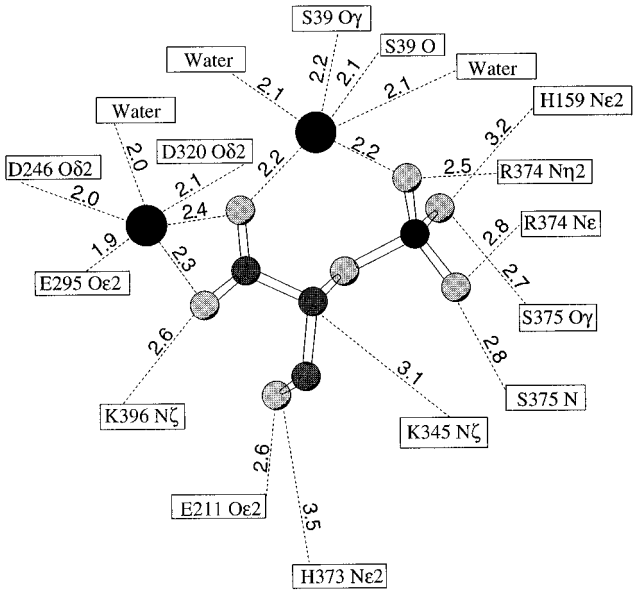

Figure III.D.1. Schematic diagram of the enolase active site residue interactions with the $(Mg^{2+})_2$–substrate/product complex. The dashed lines from 2-PGA to amino acids represent possible hydrogen bonds. The dashed lines from the magnesium ions indicate their coordination. Interatomic distances in angstroms are given on the dashed lines. From Larsen et al. (1996) with permission.

holoenzyme and both substrate and product molecules. The substrate complex is depicted in Figure III.D.1.[102] This structure reveals that both Mg^{2+} ions participate in binding the carboxylate group of 2-PGA in a μ-1,1-bridging geometry. The higher affinity Mg^{2+} site also binds the second carboxylate O atom. The inequivalence in the Mg–O(carboxylate) bond distances ($\Delta = 0.2$ Å) suggests that both Mg^{2+} ions are important for stabilization of the intermediate *aci*-carboxylate **5**. These bond lengths are quite long (2.2–2.4 Å) in comparison to bond lengths of Mg–O oxyanion complexes which fall in the range 2.00–2.12 Å.[104] It can be hypothesized that shortening of these distances upon formation of the planar *aci*-carboxylate by deprotonation at C-2 should contribute appreciably to the binding affinity of the transition state, thus lowering the activation barrier for catalysis. The lower affinity Mg^{2+} site binds directly to the phosphoryl group of substrate and product and thus appears important for substrate selectivity. Several other amino acids involved in hydrogen bonding to the substrate and product molecules undoubtedly contribute to selectivity and activity of the enzyme. Substrate binding appears to involve closing of a latch comprised of a loop from the protein that anchors to the lower affinity Mg^{2+} site by chelation to both the carbonyl O and side chain O_γ of serine 39.

The closest functional group to the C-2 carbon of the substrate molecule is the terminal Nϵ atom of a lysine residue located at 3.1 Å. This group is proposed to be the general base where the ionized proton binds following deprotonation of substrate. Relative to an unperturbed lysine group with $pK_a = 10.8$ the pK_a for deprotonation at C-2 in solution is estimated at 28–32.[105] This pK_a must be lowered in the active site in order that formation of the *aci*-carboxylate not be the rate-limiting step in the reaction. Metal coordination appears to play a major

role in accelerating this step. It was previously found on the basis of isotope exchange experiments that the second step in the reaction of eq 4, involving hydroxide release and planarization of the C2−C3 double bond is the rate-limiting step.[105] Other workers have found that product release, rather than elimination of hydroxide in the second step is likely to contribute to the rate-limiting step under steady-state turnover conditions.[106]

2. Phosphotriesterase

The hydrolysis of phosphotriesters and related phosphonates in certain bacteria is catalyzed by a metalloenzyme called phosphotriesterase. Although these substrates are not natural products, the bacterial enzymes appears to have evolved recently. They exhibit high selectivity and greatly accelerate the rate of hydrolysis with values of k_{cat} nearly 10^4 s^{-1}.[107] The enzyme is speculated to have evolved in response to toxic stress from organophosphates in the environment. The native enzyme binds two Zn^{2+} ions, but also is catalytically active with a variety of divalent ions including Cd^{2+}, Ni^{2+}, Co^{2+}, and Mn^{2+}. The dimanganese enzyme exhibits a spin-coupled binuclear center according to EPR spectroscopy.[108] A crystal structure of the $(Cd^{2+})_2$-holoenzyme has been reported which gives a model for the structure of the enzyme.[109] The separation of the Cd^{2+} ions was restrained to a distance of 3.3 Å in the model. An unusual feature of the structure is the presence of a carbamylated lysine residue that bridges between the Cd^{2+} ions in a μ-1,3 geometry and by a μ-aqua (or hydroxide) ligand. The implications of the protein structure on the mechanism of catalysis have not been described yet. A carbamylated lysine residue also bridges the pair of Ni^{2+} ions in the active site of urease.[110] It has been pointed out that a carbamylated lysine should provide a stronger ligand field than the carboxylate group of glutamate, owing to its ability to undergo proton ionization at Nϵ and delocalization of the electron pair into the bridging carboxylate.[109] Thus, one can anticipate that delivery of a proton from the Nϵ site may be a unique aspect of catalysis by enzymes containing a metal-bound carbamylated lysine residues in the active site.

3. Dinitrogen Reductase Regulatory Protein

Nitrogenase activity in the purple non-sulfur bacterium *Rhodospirillum rubrum* is regulated by the reversible ADP-ribosylation of Arg101 of the dinitrogenease reductase protein.[111] The enzymes that perform the ADP-ribosylation reaction (DRAT) and the removal of ADP-ribose (DRAG) have been overexpressed, and their roles in regulation of dinitrogenase reductase activity have been determined. DRAG is a Mn-containing enzyme. Recently it has been found to contain a dimanganese site which exhibits an EPR signal typical of the weakly spin-coupled Mn_2(II,II) type centers, like those found in arginase, catalase, and enolase.[112] The role of the dimanganese site in the hydrolytic deribosylation reaction of the protein substrate, L-arginine-ADP-ribosyl, remains to be established.

4. L-Arginine-Metabolizing Enzyme of Photosystem II

Partial characterization of a Mn-requiring enzyme associated with photosystem II complexes of spinach and tobacco has been reported.[113] The isolated protein has a molecular mass of 7 kDa and exhibits a weak activity in hydrolysis of L-arginine to urea and L-ornithine (arginase reaction) that requires Mn. The Mn stoichiometry was not established, but a second site, required for activity, binds Ca^{2+} or Mn^{2+}. The highest activity (10×) is observed in intact PSII membranes depleted of the extrinsic proteins of the water-oxidizing complex (33, 23, and 17 kDa). The protein also has a weak catalase activity which was taken to suggest a possible role in water oxidation and suggests the presence of a binuclear Mn site. The functional role of the protein is not known.

IV. Summary

Binuclear metal sites in enzymes play a number of conventional roles in catalysis. The foregoing examples illustrate cases where the two metal ions operate as a unit to accomplish one or more of the following steps: (1) activate a substrate molecule for either oxidation or reduction; (2) activate a substrate molecule for deprotonation or nucleophillic addition; (3) ionize a water molecule; (4) stabilize a transition-state intermediate; (5) molecular recognition of substrate and selectivity. Nature has evolved binuclear sites in enzymes for special purposes too. The more extended charge distribution that can be achieved with binuclear metal sites vs amino acids from a protein or nucleotides from RNA or DNA is an important factor for recognition of polyanionic substrates and for stabilization of transition states requiring charge delocalization over multiple atoms. For substrates which bind between the metal ions a larger electrical potential can be achieved without increasing unwanted activation barriers than in the analogous monometallic site.

V. Abbreviations

Arginase-Mn_2(II,II), Arg(II,II); dinitrogen reductase regulatory protein, DRAG; manganese catalase, Mn-Cat; methane monooxygenase, MMO; 2-phospho-D-glycerate, 2-PGA; phosphoenolpyruvate, P-enolpyruvate; ribonuclease H, RNase H; superoxide dismutase, SOD; zero-field splitting, ZFS.

VI. Acknowledgments

I thank my co-workers who assisted in gathering the information, drafting figures, and proofreading: Drs. Sergei Khangulov, David Ash, and Alexandra Boelrijk; Mr. Wolfgang Ruttinger, Mr. Gavin Dunn, and Ms. Kristin Larson. Research in the authors' laboratory is supported by the National Institutes of Health, under grants GM39932 and DK45414.

Note Added in Proof

An atomic model of the structure of liver arginase has been described recently, on the basis of X-ray diffraction analysis of single crystals. (Kanyo, Z. F.; Scolnick, L. R.; Ash, D. E.; Christianson, D. W. *Nature*, **1996**, in press.)

VII. References

(1) Allen, K. N.; Lavie, A.; Glasfeld, A.; Tanada, T. N.; Gerrity, D. P.; Carlson, S. C.; Farber, G. K.; Petsko, G. A.; Ringe, D. *Biochemistry* **1994**, *33*, 1488−1494.

(2) Allen, K. N.; Lavie, A.; Farber, G. K.; Glasfeld, A.; Petsko, G. A.; Ringe, D. *Biochemistry* **1994**, *33*, 1481−1487.
(3) Collyer, C. A.; Henrick, K.; Blow, D. M. *J. Mol. Biol.* **1990**, *212*, 211−235.
(4) Lavie, A.; Allen, K. N.; Petsko, G. A.; Ringe, D. *Biochemistry* **1994**, *33*, 5469−5480.
(5) Markham, G. D. In *Manganese in Metablolism and Enzyme Function*; Wedler, V. L. S. a. F. C., Ed.; Academic Press: New York, 1986.
(6) Que, L., Jr.; True, A. E. In *Prof. Inorg. Chem.: Bioinorganic Chem.*; Lippard, S. J., Ed.; John Wiley: New York, 1990; Vol. 38.
(7) *Manganese Redox Enzymes*; Pecoraro, V. L., Ed.; VCH: New York, 1992.
(8) Dismukes, G. C. In *Bioinorganic Catalysis*; Reedijk, J., Ed.; Marcel-Dekker: Amsterdam, 1992.
(9) Dismukes, G. C. In *Mixed Valency Systems: Applications in Chemistry, Physics and Biology*; Prassides, K., Ed.; Kluwer Acad. Publ.: Dordrecht,1991.
(10) Kessissoglou, D. P. *Manganese-Proteins and - Enzymes and Relevant Trinuclear Synthetic Complexes*; Kluwer: Dordrecht, 1995.
(11) Manchanda, R.; Brudvig, G. W.; Crabtreee, R. H. *Coord. Chem. Rev.* **1995**, *144*, 1−38.
(12) Pecoraro, V. L.; Baldwin, M. J.; Gelasco, A. *Chem. Rev.* **1994**, *94*, 807−826.
(13) Wieghardt, K., 1989. 28: p. 1153−1172. *Angew. Chem., Int. Ed. Engl.* **1989**, *28*, 1153−1172.
(14) Christou, G. *Acc. Chem. Res.* **1989**, *22*, 328−335.
(15) Sychev, A. Y.; Isac, V. G. *Russ. Chem. Rev. (Engl.)* **1993**, *62*, 279−290.
(16) Berry, R. S.; Rice, S. A.; Ross, J. *Physical Chemistry*; John Wiley: New York, 1980.
(17) *The Biological Chemistry of Magnesium*; Cowan, J. A., Ed.; VCH: New York, 1995.
(18) Bertini, I.; Banci, L.; Piccioli, M.; Luchinat, C. *Coord. Chem. Rev.* **1990**, *100*, 67−103.
(19) Strater, N.; Klabunde, T.; Tucker, P.; Witzel, H.; Krebs, B. *Science* **1995**, *268*, 1489−1492.
(20) Ruttinger, W.; Dismukes, G. C. *Chemical Reviews* **1996**, *submitted*.
(21) Wang, D. L.; Holz, R. C.; David, S. S.; Que, L., Jr.; Stankovich, M. T. *Biochemistry* **1991**, *30*, 8187−8194.
(22) Sossong, T. J.; Khangulov, S. V.; Cavalli, R. C.; Soprano, D. R.; Dismukes, G. C.; Ash, D. E. *Biochemistry* **1996**, *submitted*.
(23) Beese, L. S.; Steitz, T. A. *EMBO J.* **1991**, *10*, 25−33.
(24) Fothergill, M.; Goodman, M. F.; Petruska, J.; Warshel, A. *J. Am. Chem. Soc.* **1995**, *117*, 11619−627.
(25) Rosenzwweig, A. C.; Nordlund, P.; Takahara, P. M.; Frederick, C. A.; Lippard, S. J. *Chem. Biol.* **1995**, *2*, 409−418.
(26) Rardin, R. L.; Tolman, W. B.; Lippard, S. J. *New J. Chem.* **1991**, *15*, 417−430.
(27) Dismukes, G. C.; Shank, M.; Pessiki, P. J.; Khangulov, S. V.; Barynin, V. V. *J. Inorg. Biochem.* **1995**, *59*, 623 (extended abstract).
(28) Stenkamp, R. E. *Chem. Rev.* **1994**, *94*, 715−726.
(29) Paulsen, K. E.; Fox, B. G.; Lipscomb, J. D.; Munck, E.; Stankovich, M. T. *Biochemistry* **1994**, *33*, 713−722.
(30) Sturgeon, B. E.; Burdi, D.; Chen, S.; Huynh, B.-H.; Edmondson, D. E.; Stubbe, J.; Hoffman, B. M. *J. Am. Chem. Soc.* **1996**, *118*, 7551−7557.
(31) Khangulov, S. V.; Pessiki, P. J.; Barynin, V. V.; Ash, D. E.; Dismukes, G. C. *Biochemistry* **1995**, *34*, 2015−2025.
(32) Pessiki, P. J.; Dismukes, G. C. *J. Am. Chem. Soc* **1994**, *116*, 898−903.
(33) Mathur, P.; Crowder, M.; Dismukes, G. C. *J. Am. Chem. Soc.* **1987**, *109*, 5227−5232.
(34) Khangulov, S. V.; Voyevodskaya, N. V.; Barynin, V. V.; Grebenko, A. I.; Melik-Adamyan, V. R. *Biofizika (Biophysics)* **1987**, *32*, 960−966 (1044−1051 Engl.).
(35) Penner-Hahn, J. E. In *Manganese Redox Enzymes*; Pecoraro, V. L., Ed.; Verlag Chemie: New York, 1992.
(36) Shank, M. L. B.S. Thesis, Princeton, 1994.
(37) Shank, M.; Khangulov, S. V.; Barynin, V.; Dismukes, G. C. *J. Bioinorg. Chem.* **1996**, *submitted*.
(38) Herzfeld, A.; Raper, S. M. *Biochem. J.* **1976**, *153*, 469−478.
(39) Ratther, S.; Morell, H.; Cavalho, E. *Arch. Biochem. Biophys.* **1960**, *91*, 280.
(40) Reddi, P. K.; Knox, W. E.; Herzfeld, A. *Enzyme* **1975**, *20*, 305−314.
(41) Haraguchi, Y.; Takaguchi, M.; Amaya, Y.; Kawamoto, S.; Matsuda, I.; Mori, M. *Proc. Nat. Acad. Sci. U.S.A.* **1987**, *84*, 412−415.
(42) Dizikes, G. J.; Spector, E. B.; Cerbaum, S. D. *Somatic Cell. Mol. Genet.* **1986**, *12*, 375.
(43) Kawamoto, S.; Amaya, Y.; Oda, T.; Kuzumi, T.; Saheki, T.; Kimura, S.; Mori, M. *Biochem. Biophys. Res. Commun.* **1986**, *136*, 955−961.
(44) Reczkowski, R. S.; Ash, D. E. *J. Am. Chem. Soc.* **1992**, *114* (27), 10992−10994.
(45) Cavalli, R. C.; Burke, C. J.; Soprano, D. R.; Kawamoto, S.; Ash, D. E. *Biochemistry* **1994**, *33*, 10652−10657.
(46) Reczkowski, R. S.; Ash, D. E. *Arch. Biochem. Biophys.* **1994**, *312* (1), 31−37.
(47) Custot, J.; Boucher, J.-L.; Vadon, S.; Guedes, C.; Dijols, S.; DeLaforge, M.; Mansuy, D. *J. Biol. Inorg. Chem.* **1996**, *1*, 73−82.
(48) Kuhn, N. J.; Talbot, J.; Ward, S. *Arch. Biochem. Biophys.* **1991**, *286*, 217−221.
(49) Smith, R. M.; Martell, A. E. *Critical Stability Constants*; Plenum: New York, 1976.
(50) Sivaraja, M.; Stouch, T. R.; Dismukes, G. C. *J. Am. Chem. Soc.* **1992**, *114*, 9600−9602.
(51) Zheng, M.; Khangulov, S. V.; Dismukes, G. C.; Barynin, V. V. *Inorg. Chem.* **1994**, *33*, 382−387.
(52) Ishii, M.; Funabashi, S.; Tanaka, M. *Inorg. Chem.* **1998**, *27*.
(53) Cheng, Y.; Khangulov, S. V.; Sossong, T.; Cavelli, C.; Soparano, D.; Ash, D. E.; Dismukes, G. C. *J. Inorg. Biochem.* **1995**, *59 (abst.)*.
(54) Kleinfeld, D.; Okamura, M. Y.; Feher, G. *Biochim. Biophys. Acta* **1984**, *766*, 126−140.
(55) Shank, M.; Barynin, V.; Dismukes, G. C. *Biochemistry* **1994**, *33*, 15433−15436.
(56) Halliwell, B.; Gutteridge, J. M. C. In *Methods of Enzymology*; Packer, L., Glazer, A. N., Eds.; Academic Press: San Diego, 1990.
(57) Stadtman, E. R.; Berlett, P. B.; Chock, P. B. *Proc. Nat. Acad. Sci. U.S.A.* **1990**, *87*, 384−388.
(58) Barynin, V. V.; Grebenko, A. I. *Dokl. Akad. Nauk. SSSR* **1986**, *286*, 461−464.
(59) Kono, Y.; Fridovich, I. *J. Biol. Chem.* **1983**, *258*, 6015−6019.
(60) Barynin, V. V.; Vagin, A. A.; Melik-Adamyan, W. R.; Grebenko, A. I.; Khangulov, S. V.; Popov, A. N.; Andrianova, M. E.; Vainshtein, B. K. *Dokl. Akad. Nauk. SSSR [Crystallogr.]* **1986**, *288*, 877−880 (Russian).
(61) Barynin, V. V. *J. Inorg. Biochem.* **1991**, *43*, 362 (abst).
(62) deMare, F.; Kurtz, D. M., Jr.; Nordlund, P. *Nature, Struct. Biol.* **1996**, *3*, 539−546.
(63) Khangulov, S. V.; Barynin, V. V.; Melik-Adamyan, V. R.; Grebenko, A. I.; Voevodskay, N. V.; A., B. L.; Dobrykov, S. N.; Il'ysova, V. B. *Bioorgan. Khim.* **1986**, *12*, 741−748 (Russian).
(64) Khangulov, S. V.; Barynin, V. V.; Voevodskaya, N. V.; Grebenko, A. I. *Biochim. Biophys. Acta* **1990**, *1020*, 305−310.
(65) Fronko, R. M.; Penner-Hahn, J. E.; Bender, C. J. *J. Am. Chem. Soc.* **1988**, *110*, 7554−7555.
(66) Meier, A. E.; Whitaker, M. M.; Whitaker, J. W. *Biochemistry* **1996**, *35*, 348−360.
(67) Khangulov, S. V.; Goldfeld, M. G.; Gerasimenko, V. V.; Andreeva, N. E.; Barynin, V. V.; Grebenko, A. I. *J. Inorg. Biochem.* **1990**, *40*, 279−292.
(68) Grush, M. M.; Chen, J.; Stemmler, T. L.; George, S. J.; Ralston, C. Y.; Stibrany, R. T.; Gelasco, A.; Gorun, S. M.; Penner-Hahn, J. E.; Cramer, S. P. *J. Am. Chem. Soc.* **1996**, *118*, 65−69.
(69) Waldo, G. S.; Yu, S.; Penner-Hahn, J. E. *J. Am. Chem. Soc.* **1992**, *114*, 5869−5870.
(70) Gamelin, D. R.; Kirk, M. L.; Stemmler, T. L.; Pal, S.; Armstrong, W. H.; Penner-Hahn, J. E.; Solomon, E. I. *J. Am. Chem. Soc.* **1994**, *116*, 2392−2399.
(71) Khangulov, S. V.; Sivaraja, M.; V., B. V.; Dismukes, G. C. *Biochemistry* **1993**, *32*, 4912−4924.
(72) Dikanov, S. A.; Tsetkov, Y. D.; Khangulov, S. V.; Goldfeld, M. G. *Dokl. Biophy.* **1988**, *302*, 174−176 (English).
(73) Ivancich, A.; Barynin, V. V.; Zimmermann, J.-L. *Biochemistry* **1995**, *34* (20), 6628−6639.
(74) Khangulov, S. V.; Barynin, V. V.; Antonyuk-Barynina, S. V. *Biochim. Biophys. Acta* **1990**, *1020*, 25−33.
(75) Waldo, G. S.; Penner-Hahn, J. E. *Biochemistry* **1995**, *34*, 1507−1512.
(76) Khangulov, S. V.; Andreeva, N. E.; Gerasimenko, V. V.; Goldfeld, M. G.; Barynin, V. V.; Grebenko, A. I. *Russ. J. Phys. Chem.* **1990**, *64*, 10−16 (English).
(77) Sheats, J. E.; Czernuziewicz, R.; Dismukes, G. C.; Rheingold, A.; Petrouleas, V.; Stubbe, J.; Armstrong, W. H.; Beer, R.; Lippard, S. J. *J. Am. Chem. Soc.* **1987**, *109*, 1435−1444.
(78) Czernuszewicz, R. S.; Dave, B.; Rankin, J. G. *Spec. Publ. - R. Soc. Chem.* **1991**, *94*.
(79) Carroll, J. M.; Norton, J. R. *J. Am. Chem. Soc.* **1992**, *114*, 8744−8745; *115*, 12639 (correction).
(80) Hughes, S. H.; Arnold, E.; Hostomsky, Z. In *Ribonuclease H*; Toulme, R. J. C. a. J. J., Ed.; INSERM Editions: Paris, 1996.
(81) Davies, J. F.; Hostomska, Z.; Hostomsky, Z.; Jordon, S.; Mathews, D. A. *Science* **1991**, *252*, 88−95.
(82) Setlick, R. F.; Meyer, D. J.; Shibata, M.; Rostwitalski, R.; Ornstein, R. L.; Rein, R. *J. Biomol Struct. Dyn.* **1994**, *12*.
(83) Black, C. B.; Cowan, J. A. *Inorg. Chem.* **1994**, *33*, 5805−5808.
(84) Katanagi, K.; Okumura, M.; Morikawa, K. *Proteins* **1993**, *17*, 337−346.
(85) Yang, W.; Steitz, T. A. *Structure* **1995**, *3*, 131−135.
(86) Cech, T. R. A. *Rev. Biochem.* **1990**, *59*, 543−568.
(87) Pyle, A. M. *Science* **1993**, *261*, 709−714.
(88) Pley, H. W.; Flaherty, K. M.; McKay, D. B. *Nature* **1994**, *372*, 68−74.

(89) Scott, W. G.; Finch, J. T.; Klug, A. *Cell* **1995**, *81*, 991−1002.
(90) Sawata, S.; Komiyama, M.; Taira, K. *J. Am. Chem. Soc.* **1995**, *117*, 2357−2358.
(91) Dahm, S. C.; Derrick, W. B.; Uhlenbeck, O. C. *Biochemistry* **1993**, *32*, 13040−13045.
(92) Hertel, K. J.; Uhlenbeck, O. C. *Biochemistry* **1995**, *34*, 1744−1749.
(93) Piccirilli, J. A.; Vyle, J. S.; Caruthers, M. H.; Cech, T. R. *Nature* **1993**, *361*, 85−88.
(94) Kuimelis, R. G.; McLaughlin, L. W. *Biochemistry* **1996**, *35*, 5308−5317.
(95) Zhou, D.-M.; Usman, N.; Wincott, F. E.; Matulic-Adamic, J.; Komiyama, M.; Kumar, P. K. R.; Taira, K. *J. Am. Chem. Soc.* **1996**, *118*, 5862−5866.
(96) Sigel, H. *Coord. Chem. Rev.* **1990**, *100*, 453−539.
(97) Gerlt, J. A.; Gassman, P. G. *Biochemistry* **1993**, *32*, 11943−11952.
(98) Wedekind, J. E.; Poyner, R. R.; Reed, G. H.; Rayment, I. *Biochemistry* **1994**, *33*, 9333−9342.
(99) Walsh, C. *Enzymatic Reaction Mechanisms*; W. H Freeman: San Francisco, 1979.
(100) Poyner, R. R.; Reed, G. H. *Biochemistry* **1992**, *31*, 7166−7173.
(101) Lebioda, L.; Stec, B. *Biochemistry* **1991**, *30*, 2817−2822.
(102) Larsen, T. M.; Wedekind, J. E.; Rayment, I.; Reed, G. H. *Biochemistry* **1996**, *35*, 4349−4358.
(103) Duquerroy, S.; Camus, C.; J., J. *Biochemistry* **1995**, *34*, 12513−12523.
(104) Frausto, J. J. R.; Williams, R. J. P. *The Biological Chemistry of the Elements*; Clarendon Press: Oxford, 1991.
(105) Dinovo, E. C.; Boyer, P. D. *J. Biol. Chemistry* **1971**, *246*, 4586−4593.
(106) Shen, O.; Westhead, E. W. *Biochemistry* **1973**, *12*, 3333−39.
(107) Omburo, G. A.; Mullins, L. S.; Raushel, F. M. *J. Biol. Chem.* **1992**, *267*, 13278−13283.
(108) Chae, M. Y.; Omburo, G. A.; Lindahl, P.; Raushel, F. M. *J. Am. Chem. Soc.* **1993**, *115*, 12173−12174.
(109) Benning, M.; Kuo, J. M.; Raushel, F. M.; Holden, H. M. *Biochemistry* **1995**, *34*, 7973−7978.
(110) Jabri, E.; Carr, M. B.; Hausinger, R. P.; Karplus, P. A. *Science* **1995**, *268*, 998−1001.
(111) Ludden, P. W.; Roberts, G.; Grunwald, S.; Lies, D.; Nielsen, G. VIII International Symposium on Phototrophic Prokaryotes, Urbino, Italy, 1994; abstract, p 54.
(112) Ludden, P. W. Personal commun.
(113) Gau, A. E.; Thole, H. H.; Pistorius, E. K. *Z. Naturforsch.* **1995**, *50 C*, 638.
(114) Allgood, G. S.; Perry, J. J. *J. Bacteriol.* **1986**, *168*.

CR950053C